Title no. 105-S42

Punching Shear Strength of Reinforced Concrete Slabs without Transverse Reinforcement

by Aurelio Muttoni

A mechanical explanation of the phenomenon of punching shear in slabs without transverse reinforcement is presented on the basis of the opening of a critical shear crack. It leads to the formulation of a new failure criterion for punching shear based on the rotation of a slab. This criterion correctly describes punching shear failures observed in experimental testing, even in slabs with low reinforcement ratios. Its application requires the knowledge of the load-rotation relationship of the slab, for which a simple mechanical model is proposed. The resulting approach is shown to give better results than current design codes, with a very low coefficient of variation (COV). Parametric studies demonstrate that it correctly predicts several aspects of punching shear previously observed in testing as size effect (decreasing nominal shear strength with increasing size of the member). Accounting for the proposed failure criterion and load-rotation relationship of the slab, the punching shear strength of a flat slab is shown to depend on the span of the slab, rather than on its thickness as often proposed.

Keywords: critical shear crack; interior slab-column connection; punching shear; two-way shear.

INTRODUCTION

Reinforced concrete slabs on columns were initially developed in the U.S. and Europe at the beginning of the 20th century.[1,2] Their designs typically included large mushroom-shaped column capitals to facilitate the local introduction of forces from the slab to the column. In the 1950s, flat slabs without capitals started to become prevalent. Because of their simplicity, both for construction and for use (simple formwork and reinforcement, flat soffit allowing an easy placement of equipment, and installation underneath the slab), they have become very common for medium height residential and office buildings as well as for parking garages. The design of flat slabs is mostly governed by serviceability conditions on the one side (with relatively large deflections in service) and by the ultimate limit state of punching shear (also called two-way shear) on the other side. These two criteria typically lead to the selection of the appropriate slab thickness.

Punching shear has been the object of an intense experimental effort since the 1950s. In most cases, the phenomenon is investigated by considering an isolated slab element. This element typically represents the surface of the slab surrounding a column and is delimited by the line of contraflexure for radial moments, which are zero at a distance $r_s \approx 0.22L$ (according to a linear-elastic estimate), where L is the axis-to-axis spacing of the columns. In recent years, several state-of-the-art reports and synthesis papers have been published on this topic.[3-5]

Most design codes base their verifications on a critical section, with the punching shear strength of slabs without shear reinforcement defined as a function of the concrete compressive strength and often of the reinforcement ratio. Some codes also account for size effect, membrane effect, or the ratio of column size to the depth of the slab. Equation (1) shows the ACI 318-05[6] expression for square or circular columns of moderate dimensions relative to the thickness of the slab

$$V_R = \frac{1}{3} b_0 d \sqrt{f_c'} \quad \text{(SI units: MPa, mm)}$$
$$V_R = 4 b_0 d \sqrt{f_c'} \quad \text{(U.S. customary units: psi, in.)} \tag{1}$$

where d is the average flexural depth of the slab, b_0 is the perimeter of the critical section located $d/2$ from the face of the column, and f_c' is the specified concrete compressive strength.

The current version of Eurocode 2[7] also includes a formulation for estimating the punching shear strength of slabs

$$V_R = 0.18 b_0 d \xi (100 \rho_l f_c')^{\frac{1}{3}} \quad \text{(SI units: MPa, mm)}$$
$$V_R = 5.0 b_0 d \xi (100 \rho_l f_c')^{\frac{1}{3}} \quad \text{(U.S. customary units: psi, in.)} \tag{2}$$

where b_0 is the control perimeter located $2d$ from the face of the column, ρ_l accounts for the bending reinforcement ratio (with a maximum value of 0.02) and ξ is a factor accounting for size effect defined by the following expression

$$\xi = 1 + \sqrt{\frac{200 \text{ mm}}{d}} = 1 + \sqrt{\frac{7.87 \text{ in.}}{d}} \le 2.0 \tag{3}$$

In the early 1960s, Kinnunen and Nylander[8] tested a series of slabs in punching, varying amongst other parameters the amount of flexural reinforcement in the slab (refer to Fig. 1). The following observations can be made from the load-rotation relationships of the tests:

- For low reinforcement ratios (test with $\rho = 0.5\%$), the observed behavior is ductile, with yielding of the entire flexural reinforcement, as illustrated by the horizontal asymptote of the load-rotation curve. In this case, the strength of the slab is limited by its flexural capacity and punching occurs only after large plastic deformations. The punching failure at the end of the plastic plateau remains brittle and leads to a sudden drop in strength;

ACI Structural Journal, V. 105, No. 4, July-August 2008.
MS No. S-2006-478 received December 11, 2006, and reviewed under Institute publication policies. Pertinent discussion including author's closure, if any, will be published in the May-June 2009 *ACI Structural Journal* if the discussion is received by January 1, 2009.

ACI member **Aurelio Muttoni** *is a Professor and Head of the Structural Concrete Laboratory at the Ecole Polytechnique Fédérale de Lausanne (EPFL), Lausanne, Switzerland. He received his diploma and PhD in civil engineering from the Swiss Federal Institute of Technology, Zurich, Switzerland, in 1982 and 1989, respectively. His research interests include the theoretical basis of the design of reinforced concrete structures, shear and punching shear, fiber-reinforced high-strength concrete, soil-structure interaction, and the conceptual design of bridges.*

- For intermediate reinforcement ratios (tests with ρ = 1.0%/0.5% and 1.0%), some yielding of the reinforcement is present in the immediate vicinity of the column, but punching occurs before yielding of the entire slab reinforcement. In this case, the strength of the slab is lower than its flexural capacity;
- For large reinforcement ratios (test with ρ = 2.1%/1.0%), punching occurs before any yielding of the reinforcement takes place, in a very brittle manner. In this case, the strength of the slab is significantly lower than its flexural capacity;
- Increasing the reinforcement ratio increases the punching capacity, but strongly decreases the deformation capacity of the slab; and
- The ACI design equation is also plotted in the figure. It predicts a constant strength independent from the reinforcement ratio. As observed by Alexander and Hawkins,[9] Eq. (1) is basically a design equation; as such, it does not account for the effect of the flexural reinforcement.

On the basis of their test results, Kinnunen and Nylander[8] developed a rational theory for the estimation of the punching shear strength in the early 1960s based on the assumption that the punching strength is reached for a given critical rotation ψ. This rotation was calculated by simplifying the kinematics of the slab and assuming a bilinear moment-curvature relationship. Thus far, this proposal remains one of the best models for the phenomenon of punching. Recently, some improvements were proposed by Hallgren[10] and Broms[11] to account for size effects and high-strength concrete. While very elegant and leading to good results, this model was never directly included in codes of practice because its application is too complex. It served as a basis, however, for the Swedish and Swiss design codes of the 1960s.

RESEARCH SIGNIFICANCE

Rational models and design formulas for punching shear, or two-way shear, are based on the results of experimental tests performed mostly on thin slabs (*d* = 0.1 to 0.2 m [4 to 8 in.]). Design codes, however, are generally also applicable to thick slabs and footings (0.4 m [16 in.] and more). The few available tests performed on thick slabs exhibit a notable size effect. As a consequence, there is a need for a rational model correctly describing punching shear and accounting for size effect (defined as decreasing nominal shear strength with increasing size of the member).

In this paper, a new failure criterion for punching shear based on the critical shear crack theory is presented. This criterion describes the relationship between the punching shear strength of a slab and its rotation at failure, it is consistent with the works of Kinnunen and Nylander[8] and it accounts for size effect. The resulting equations are presented in a code-friendly formulation.

FAILURE CRITERION BASED ON CRITICAL SHEAR CRACK THEORY

Critical shear crack theory

As shown in Fig. 1, the punching shear strength decreases with increasing rotation of the slab. This has been explained by Muttoni and Schwartz[12] as follows: the shear strength is reduced by the presence of a critical shear crack that propagates through the slab into the inclined compression strut carrying the shear force to the column (Fig. 2(b)). Some evidences supporting the role of the shear critical crack in the punching shear strength are detailed in the following:

1. It has been shown experimentally[8,13] that the radial compressive strain in the soffit of the slab near the column, after reaching a maximum for a certain load level, begins to decrease (Fig. 2(d)). Shortly before punching, tensile strains may be observed. This phenomenon can be explained by the development of an elbow-shaped strut with a horizontal tensile member along the soffit due to the development of the critical shear crack[12] (Fig. 2(c)). A similar phenomenon has been observed in beams without shear reinforcement[12]; and

2. Experimental results by Bollinger[14] also confirm the role of the critical shear crack in the punching strength of slabs. The tested slab shown in Fig. 3(b) was reinforced by concentric rings placed at the boundary of the slab element only. With this particular reinforcement layout, only radial cracks developed and the formation of circular cracks in the critical region was avoided. Thus, the punching shear strength of this test was significantly larger than that of a similar slab with an additional ring in the critical region (Fig. 3(c)). For this test, the presence of an additional ring in the vicinity of the critical region initiated the development of a crack in that region, with a subsequent reduction of the punching shear strength of approximately 43%.

Punching shear strength as function of slab rotation

The opening of the critical shear crack reduces the strength of the inclined concrete compression strut carrying shear and eventually leads to the punching shear failure. According to Muttoni and Schwartz,[12] the width of the critical crack can be assumed to be proportional to the product ψ*d* (Fig. 4), leading to a semi-empirical failure criterion formulated in 1991 as

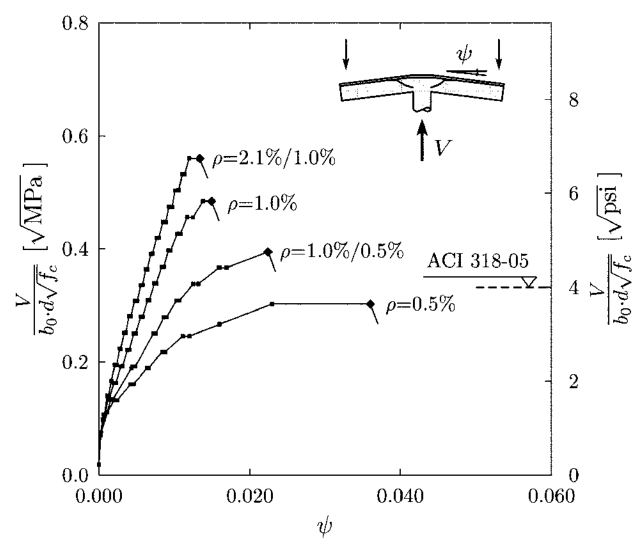

Fig. 1—Plots of load-rotation curves for tests by Kinnunen and Nylander[8] (geometric and mechanical parameters of tests defined in Fig. 8).

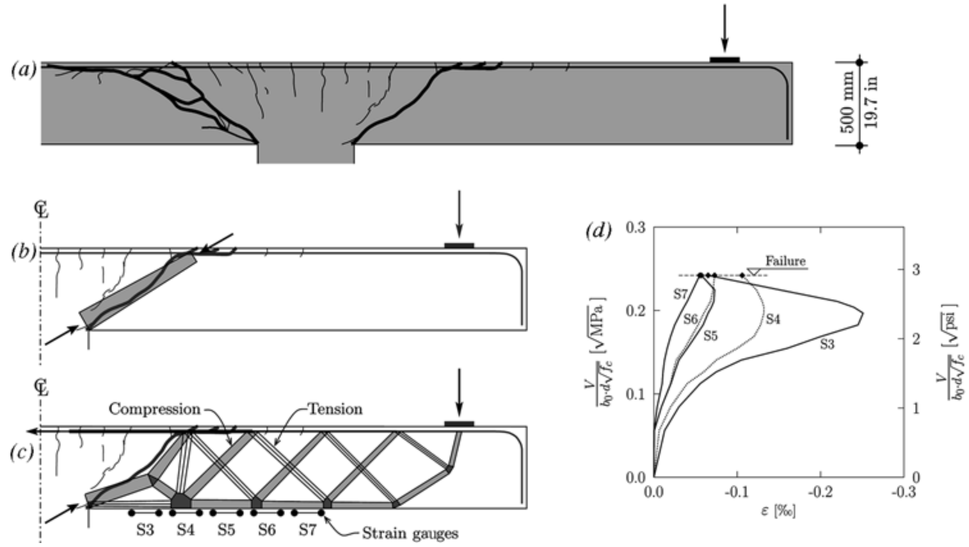

Fig. 2—Test PG-3 by Guandalini and Muttoni[13] (geometric and mechanical parameters of test defined in Fig. 9): (a) cracking pattern of slab after failure; (b) theoretical strut developing across the critical shear crack; (c) elbow-shaped strut; and (d) plots of measured radial strains in soffit of slab as function of applied load.

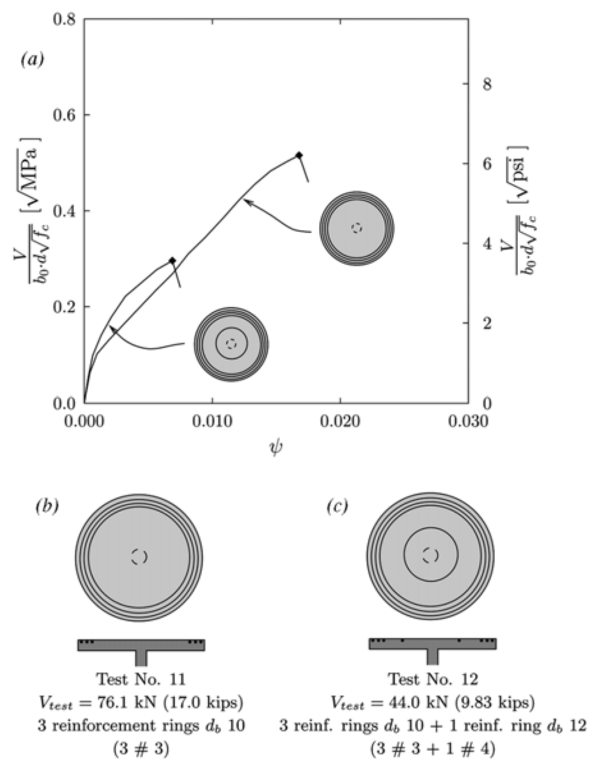

Fig. 3—Tests by Bollinger[14] with ring reinforcements, effect of additional reinforcement in vicinity of critical shear crack on load-carrying capacity: (a) test results; and (b) and (c) reinforcement layout of Specimens 11 and 12.

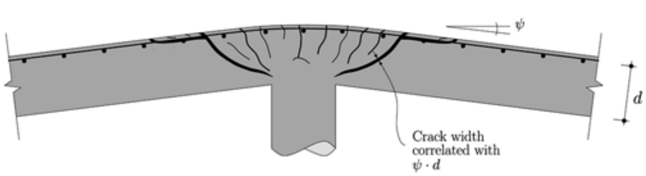

Fig. 4—Correlation between opening of critical shear crack, thickness of slab, and rotation ψ.

$$\frac{V_E}{b_0 d \sqrt[3]{f_c}} = \frac{1}{1 + \left(\frac{\psi d}{4\,\text{mm}}\right)^2} \quad \text{(SI units; N, mm)}$$

$$\frac{V_R}{b_0 d \sqrt[3]{f_c}} = \frac{28}{1 + \left(\frac{\psi d}{0.16\text{ in.}}\right)^2} \quad \text{U.S. customary units; psi, in.)} \tag{4}$$

The amount of shear that can be transferred across the critical shear crack depends on the roughness of the crack, which in its turn is a function of the maximum aggregate size. According to Walraven[15] and Vecchio and Collins,[16] the roughness of the critical crack and its capacity to carry the shear forces can be accounted for by dividing the nominal crack width ψd by the quantity $(d_{g0} + d_g)$, where d_g is the maximum aggregate size, and d_{g0} is a reference size equal to 16 mm (0.63 in.). It should be noted that the value of d_g has to be set to zero for lightweight aggregate concrete to account for cracks developing through aggregates. On that basis, in 2003 Muttoni[17] proposed an improved formulation for the failure criterion

$$\frac{V_R}{b_0 d \sqrt{f_c}} = \frac{3/4}{1 + 15\frac{\psi d}{d_{g0} + d_g}} \quad \text{(SI units: N, mm)}$$

$$\frac{V_R}{b_0 d \sqrt{f_c}} = \frac{9}{1 + 15\frac{\psi d}{d_{g0} + d_g}} \quad \text{(U.S. customary units: psi, in.)} \tag{5}$$

Figure 5 compares the results obtained with Eq. (5) to the results of 99 punching tests from the literature, for which Table 1 provides additional information. In this figure, the slab rotation was either obtained from direct measurements or calculated by the author from the measured deflection, assuming a conical deformation of the slab outside the column region. In cases where different reinforcement ratios were placed along orthogonal directions, the maximum rotation of the slab was considered. The rotation ψ is multiplied by the factor $d/(d_{g0} + d_g)$ to cancel the effects of slab thickness and aggregate size. Tests in which punching shear failure occurred after reaching the flexural strength V_{flex} are also considered (shown as empty squares in the figure).

The expression provided in ACI 318-05[6] is also plotted in Fig. 5. It can be noted that for small values of $\psi d/(d_{g0} + d_g)$, the code gives rather conservative results. This is also the area of the plot in which the majority of the tests are located. For large values of $\psi d/(d_{g0} + d_g)$, however, the ACI equation predicts significantly larger punching shear strengths than effectively observed in tests. This fact can be traced back to two causes:

1. When the ACI formula was originally proposed in the early 1960s,[9,19] only tests with relatively small effective depths were available and the influence of size effect was thus not apparent; and

2. Tests in which punching failure occurred after reaching the flexural strength but with limited rotation capacity are considered in the comparison (empty squares).

LOAD-ROTATION RELATIONSHIP

Comparing Fig. 1 and 5, it is clear that the punching failure occurs at the intersection of the load-rotation curve of the slab with the failure criterion. To enable a calculation of the punching shear strength according to Eq. (5), the relationship between the rotation ψ and the applied load V needs to be known. In the most general case, the load-rotation relationship can be obtained by a nonlinear numerical simulation of the flexural behavior of the slab, using, for example, a nonlinear finite element code. In axisymmetric cases, a numerical integration of the moment-curvature relationship can be performed directly.[26] This allows to account for bending moment redistributions in flat slabs and to account for the increase on punching shear strength due to in-plane confinement given by the flat slab in the portions of the slab near columns.[26]

The axisymmetric case of an isolated slab element can also be treated analytically after some simplifications. As already described, the tangential cracks and the radial curvature are concentrated in the vicinity of the column. Outside the critical shear crack, located at a radius r_0 (assumed to be at a distance d from the face of the column), the radial moment, and thus the radial curvature, decreases rapidly as shown in Fig. 6(d) and (e). Consequently, it can be assumed that the corresponding slab portion deforms following a conical shape with a constant slab rotation ψ (Fig. 6(a)).

In the region inside the radius r_0, the radial moment is considered constant because the equilibrium of forces is performed along cross sections defined by the shape of the inclined cracks (Fig. 6(b) and (c)), where the force in the reinforcement remains constant (due to the fact that the shear force is introduced in the column by an inclined strut developing from outside the shear critical crack (Fig. 2(b) and (c)).

The full development of the expressions for the load-rotation relationship of the slab is given in Appendix 1.* Considering a quadrilinear moment-curvature relationship for the reinforced concrete section (Fig. 7), the following expression results

$$V = \frac{2\pi}{r_q - r_c}\left(\begin{array}{c} -m_r r_0 + m_R\langle r_y - r_0\rangle + EI_1\psi\langle \ln(r_1) - \ln(r_y)\rangle + \\ EI_1\chi_{TS}\langle r_1 - r_y\rangle + m_{cr}\langle r_{cr} - r_1\rangle + EI_0\psi\langle \ln(r_s) - \ln(r_{cr})\rangle \end{array}\right) \quad (6)$$

where m_r is the radial moment per unit length acting in the slab portion at $r = r_0$ and the operator $\langle x\rangle$ is x for $x \geq 0$ and 0 for $x < 0$.

A simpler moment-curvature relationship can be adopted by neglecting the tensile strength of concrete f_{ct} and the effect of tension stiffening, leading to a bilinear relationship similar to that of Kinnunen and Nylander,[8] shown as a dotted line in Fig. 7. The analytical expression describing the load-rotation relationship is thus

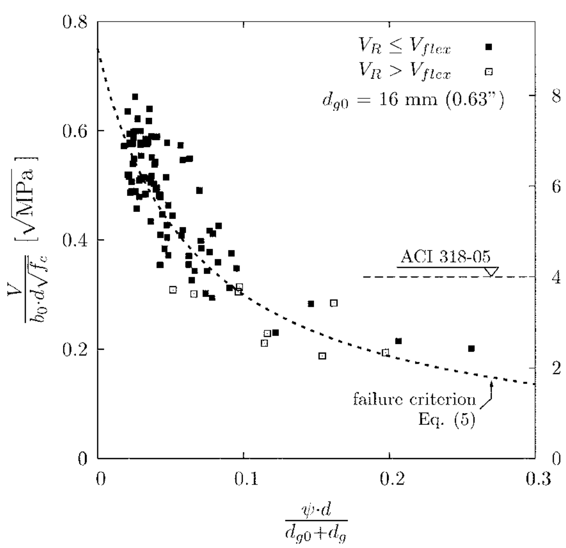

Fig. 5—Failure criterion: punching shear strength as function of width of critical shear crack compared with 99 experimental results and ACI 318-05[6] design equation, refer to details of test series in Table 1.

Table 1—Test series considered in present study and comparison with proposed failure criterion

Reference (year)	d, mm (in.)	No.	Failure criterion V_{test}/V_{th} Average	COV
Tests with same bending reinforcement ratio along orthogonal directions				
Elstner and Hognestad[18] (1956)	115 (4.52)	22	0.98	0.14
Kinnunen and Nylander[8] (1960)	122 (4.80)	12	1.05	0.11
Moe[19] (1961)	114 (4.48)	9	1.13	0.16
Schäfers[20] (1984)	113 to 170 (4.45 to 6.69)	4	1.03	0.20
Tolf[21] (1988)	98 to 200 (3.86 to 7.87)	8	1.06	0.15
Hassanzadeh[22] (1996)	200 (7.87)	3	0.99	0.17
Hallgren[10] (1996)	199 (7.83)	7	0.98	0.25
Ramdane[23] (1996)	98 (3.86)	12	1.10	0.16
Guandalini and Muttoni[13] (2004)	96 to 464 (3.78 to 18.2)	10	1.11	0.22
Σ		87	1.05	0.16
Tests with different bending reinforcement ratio along orthogonal directions				
Nylander and Sundquist[24] (1972)	95 to 202 (3.74 to 7.95)	11	1.04	0.09
Kinnunen et al.[25] (1980)	673 (26.5)	1	0.85	—
Σ		12	1.03	0.10

Note: COV = coefficient of variation.

*The Appendixes are available at **www.concrete.org** in PDF format as an addendum to the published paper. It is also available in hard copy from ACI headquarters for a fee equal to the cost of reproduction plus handling at the time of the request.

$$V = \frac{2\pi}{r_q - r_c} EI_1 \psi \left(1 + \ln\frac{r_s}{r_0}\right) \text{ for } r_y \le r_0 \text{ (elastic regime)} \quad (7a)$$

$$V = \frac{2\pi}{r_q - r_c} EI_1 \psi \left(1 + \ln\frac{r_s}{r_y}\right) \text{ for } r_0 \le r_y \le r_s \text{ (elasto-plastic regime)} \quad (7b)$$

The flexural strength of the slab specimen is reached when the radius of the yielded zone (r_y) equals the radius of the slab r_s. In this case ($r_y = r_s = r_1 = r_{cr}$, and $-m_r = m_R$), Eq. (6) yields

$$V_{flex} = 2\pi m_R \frac{r_s}{r_q - r_c} \text{ (plastic regime)} \quad (7c)$$

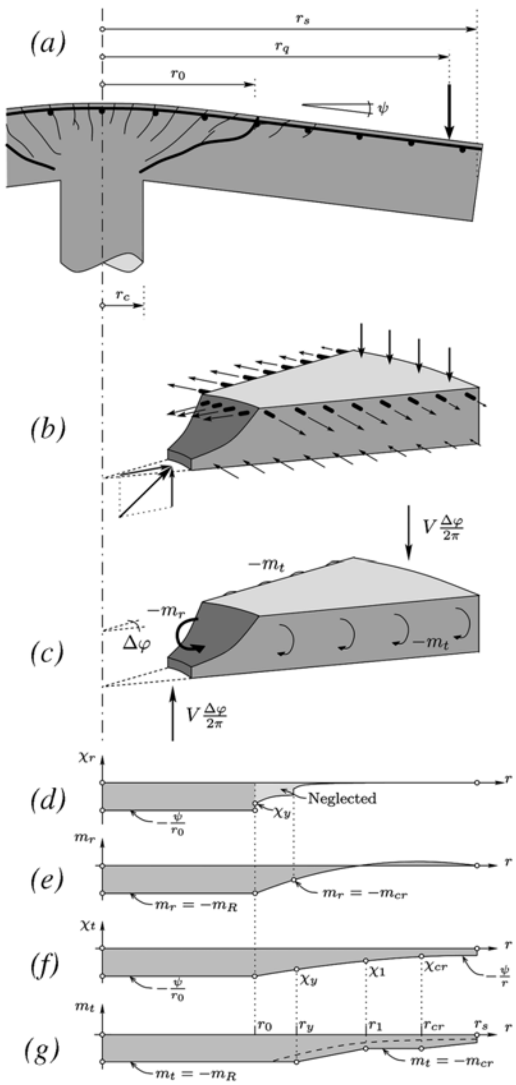

Fig. 6—Assumed behavior for axisymmetric slab: (a) geometrical parameters and rotation of slab; (b) forces in concrete and in reinforcement acting on slab sector; (c) internal forces acting on slab sector; (d) distribution of radial curvature; (e) distribution of radial moment; (f) distribution of tangential curvature; and (g) distribution of tangential moments for quadrilinear moment-curvature relationship (shaded area) and for bilinear moment-curvature relationship (dashed line).

Figure 8 shows a comparison of the proposed solutions with the previously described tests by Kinnunen and Nylander[8] (Fig. 1). The solid curves represent the solution

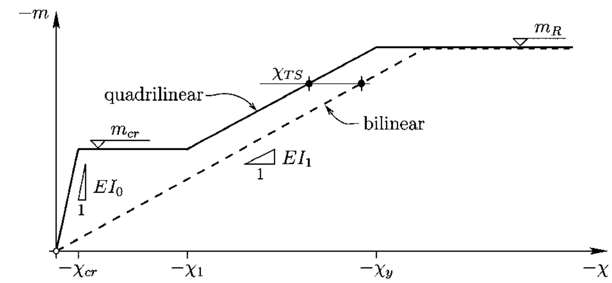

Fig. 7—Moment-curvature relationships: bilinear and quadrilinear laws.

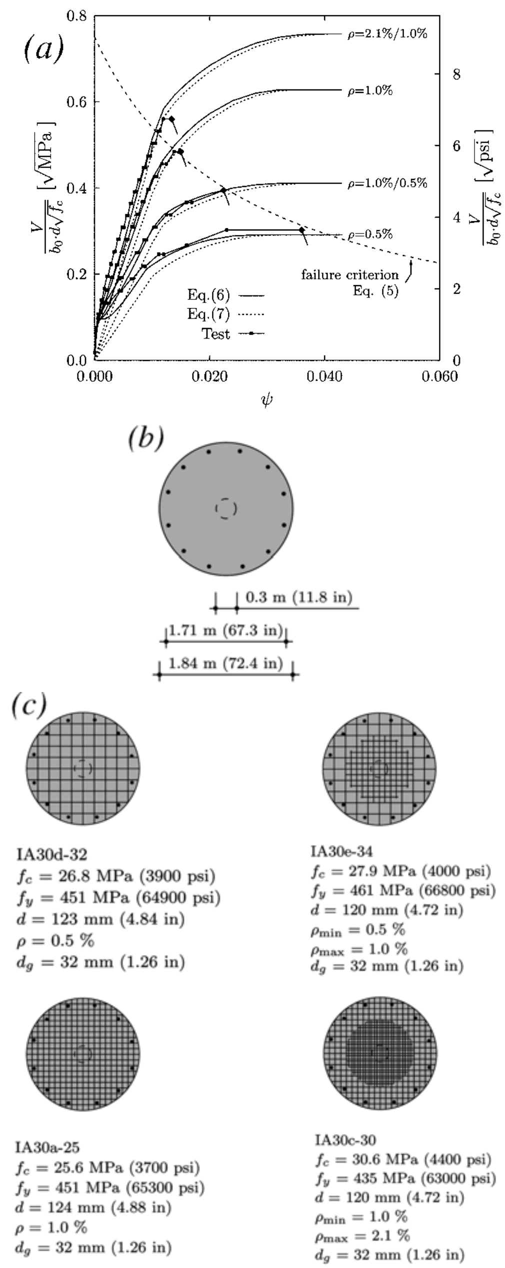

Fig. 8—Tests by Kinnunen and Nylander[8]: (a) comparison of load-rotation curves for tests and for proposed analytical expressions (Eq. (6) and (7)); (b) dimensions of specimens; and (c) mechanical parameters.

with a quadrilinear moment-curvature relationship of Eq. (6), whereas the dotted curves show the simplified solution with a bilinear moment-curvature relationship of Eq. (7). For the thin slabs of Fig. 8, both solutions predict the punching load for all reinforcement ratios very well. It may be noted, however, that the distance between the two solutions is larger for smaller reinforcement ratios at lower load levels. In these cases, Eq. (6) (which uses a quadrilinear moment-curvature relationship) predicts the full load-rotation relationship with good accuracy. Equation (7), with a simplified bilinear moment-curvature relationship, gives adequate but less accurate results, especially for low load levels, in which the tensile strength of concrete and tension stiffening effects are more pronounced. Both approaches correctly describe the actual rotation capacity of the slab at failure. The punching shear strength can be obtained directly by substituting Eq. (6) or (7) into Eq. (5) and solving the resulting equation.

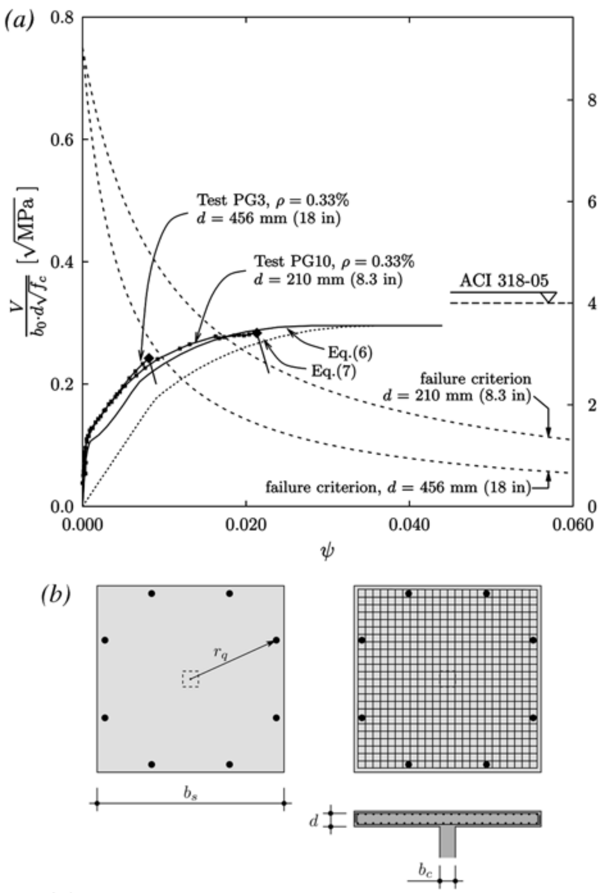

(c)

	PG – 3	PG – 10
b_s [mm (in)]	6000 (236)	3000 (118)
b_c [mm (in)]	520 (20.4)	260 (10.2)
r_q [mm (in)]	2845 (112)	1423 (56)
d [mm (in)]	456 (17.9)	210 (8.26)
ρ [%]	0.33	0.33
f_c [MPa (psi)]	32.4 (4700)	34.7 (5000)
f_y [MPa (ksi)]	520 (75.3)	577 (83.6)

Fig. 9—Load-rotation curves and failure criterion, comparison for Tests PG-3 and PG-10 by Guandalini and Muttoni[13]: (a) analytical and experimental load-rotation curves and failure criterion according to Eq. (5); (b) geometry of specimens; and (c) geometric and mechanical parameters for each specimen.

Influence of thickness of slab

Figure 9 shows the load-rotation curves for two tests by Guandalini and Muttoni.[13] These two tests are very similar, with the same reinforcement ratio (ρ = 0.33%) and the same maximum aggregate size (d_g = 16 mm [0.63 in.]). What distinguishes them is the dimensions of the slabs: Slab PG10 is 3.0 x 3.0 x 0.25 m (118 x 118 x 9.8 in.), whereas Slab PG3 is twice as large 6.0 x 6.0 x 0.5 m (236 x 236 x 19.7 in.). To facilitate the comparison of these two tests, the abscissa, contrary to the previous figures, shows the actual slab rotation, not the value corrected for aggregate size and size effect. In this representation, the load-rotation relationship of both slabs is nearly identical, as they are geometrically identical, but scaled 2:1. The failure criteria, however, are different due to their different thicknesses. This is why two dotted lines are shown, giving the failure criterion of Eq. (5) for each slab thickness, the upper applying to the thinner and the lower to the thicker slab. In the latter case, with a low reinforcement ratio, the difference between the two load-rotation relationships, with and without tension stiffening, becomes apparent, whereas the more accurate expression of Eq. (6) quite closely predicts the entirety of the loading curve, the simpler solution of Eq. (7) clearly underestimates the stiffness of the slab in its initial loading stages, thus leading to an underestimation of the punching shear strength. Whereas both equations give conservative estimates of the actual failure load, only Eq. (6) correctly describes all stages of the actual behavior of the thick slab with a small reinforcement ratio. Because both slabs are geometrically similar and because of size effect, the thicker slab has a lower rotation capacity and fails in a rather brittle manner, in spite of its low reinforcement ratio, whereas the thinner slab exhibits a more ductile behavior.

Figure 10 further illustrates this phenomenon by showing the load-rotation curves according to Eq. (6) for various reinforcement ratios, along with the failure criteria for various slab thicknesses. The constant value predicted by the ACI 318-05[6] design equation is also shown for comparison.

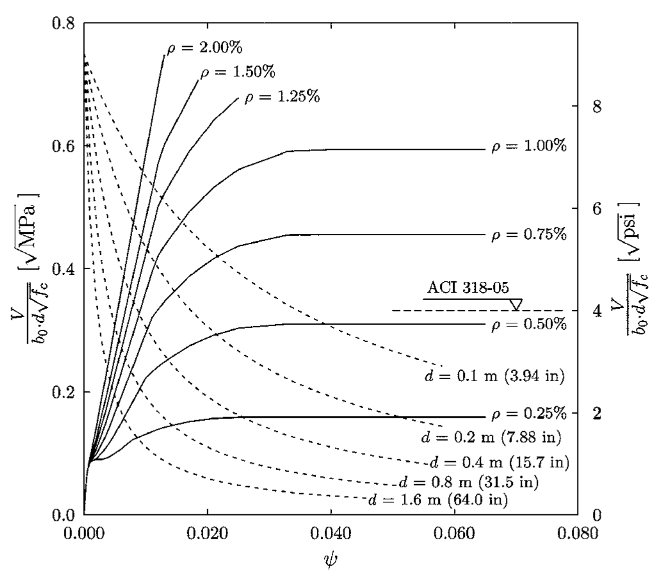

Fig. 10—Load-rotation curves and failure criteria for various reinforcement ratios and slab thicknesses ($h = r_c = 1.2d$*,* $r_s = r_q = 7d$*,* f_c *= 30 MPa [4200 psi],* f_y *= 500 MPa [71 ksi], and* d_g *= 25 mm [1 in.]).*

For thinner slabs and larger reinforcement ratios, the mode of failure is brittle, generally at values larger than predicted by the ACI equation. For lower reinforcement ratios, but in particular for thicker slabs, the equations proposed herein predict much lower values. This is especially important for thick slabs and foundation mats that may commonly exceed a thickness of 0.4 m (16 in.). In such cases, even for relatively low reinforcement ratios, the failure mode is brittle and occurs at load levels clearly below those predicted by ACI, not reaching the theoretical flexural failure load.

Moe's[19] design equation, which remains the basis for the current ACI design equation (Eq. (1)), does not include a term to account for the effect of the longitudinal reinforcement. It was, however, derived from an analytical expression that does, as explained by Alexander and Hawkins.[9] It expresses the punching shear strength as a function of the ratio V_R/V_{flex} (punching shear strength V_R to the load corresponding to the bending capacity V_{flex} of the slab). Using Eq. (7c), the test series by Moe[19] and Elstner and Hognestad[18] can be represented as in Fig. 11. From the data available at that time, Moe's[19] conclusion of a linear relationship between the punching shear strength and the ratio V_R/V_{flex} of the slab is confirmed. Shown alongside in the figure as continuous lines are the ultimate loads obtained using the proposed model. It can be observed that the level of shear at which failure occurs diminishes with increasing thickness of the slab, but the slope remains approximately the same as that observed by Moe[19] on thin slabs. The size effect is very marked, especially for thick slabs. For slabs thicker than 0.4 m (16 in.), the ACI 318-05[6] design equation overestimates the punching shear strength and does not ensure a ductile behavior.

Also shown in Fig. 11 is the effect of the bending reinforcement: increasing this reinforcement increases the punching shear capacity but simultaneously decreases the ratio of the punching load to the flexural load, which translates into smaller rotations at failure. In such cases, the only way to ensure a ductile behavior of the slab is to include shear reinforcement.

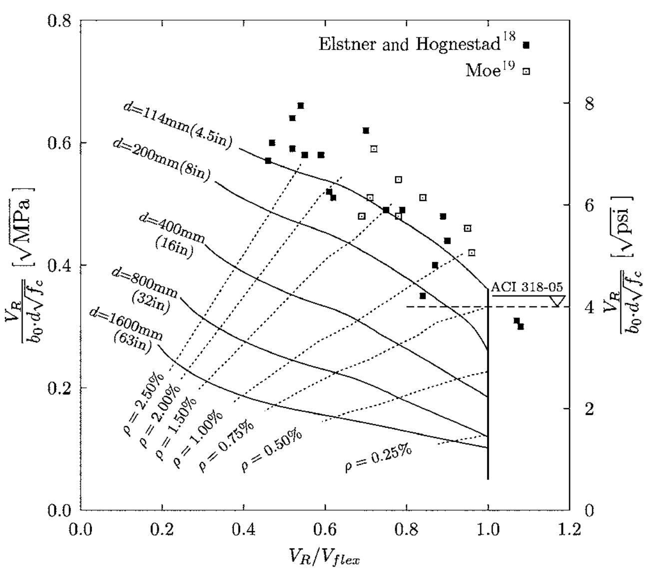

Fig. 11—Punching shear strength as function of V/V_{flex} *ratio for various slab thicknesses and reinforcement ratios* ($r_c = 1.4d$, $r_s = 9.2d$, $r_q = 7.8d$, $f_c = 24$ *MPa [3400 psi], and* $f_y = 350$ *MPa [50 ksi]); comparison with tests by Elstner and Hognestad[18] and Moe[19]* ($d = 114$ *mm [4.5 in.],* $b_c = 254$ *mm [10 in.],* $b_s = 1830$ *mm [72 in.],* $r_q = 890$ *mm [35 in.],* $f_c = 13$ *to 51 MPa [1820 to 7180 psi],* $f_y = 303$ *to 482 MPa [43.1 to 68.6 ksi], and* $\rho = 0.5$ *to 7%).*

SIMPLIFIED DESIGN METHOD

For practical purposes, the load-rotation relationship can be further simplified by assuming a parabola with a 3/2 exponent for the rotation ψ as a function of the ratio V/V_{flex} and by assuming that the flexural strength V_{flex} (refer to Eq. (7c)) is reached for a radius of the yielded zone r_y equal to 0.75 times the radius of the isolated slab element r_s. These assumptions, together with Eq. (16), (18), and (22) from Appendix 1, lead to the following relationship

$$\psi = 1.5\frac{r_s}{d}\frac{f_y}{E_s}\left(\frac{V}{V_{flex}}\right)^{3/2} \tag{8}$$

Figure 12 shows, again for the four tests by Kinnunen and Nylander,[8] the experimental load-rotation relationship along with those given by Eq. (6) and by the simplified design method of Eq. (8). Both expressions correctly predict the punching load, the simplified design equation giving slightly more conservative values.

In Table 2, the various expressions proposed in this paper, the complete solution of Eq. (6), and the simplified solution of Eq. (8) are compared on the basis of nine test series by various researchers, for a total of 87 tests. The number of tests in Table 2 is smaller than that of Table 1 because tests with different reinforcement ratios in orthogonal directions are not considered (tests by Nylander and Sundquist[24] and Kinnunen et al.[25]). For tests with square columns, the radius of the column was assumed to be $r_c = 2b_c/\pi$, where b_c is the side of the square column, leading to the same control perimeter. It should be noted that a control perimeter with rounded edges is adopted when checking the punching shear strength according to ACI 318-05[6] (this is the default control perimeter according to this code, where it is also permitted a four straight-sided control perimeter, refer to Section 11.12.1.3 of ACI 318-05[6]). Similarly, square slabs are transformed into circular elements with the same flexural strength. Also

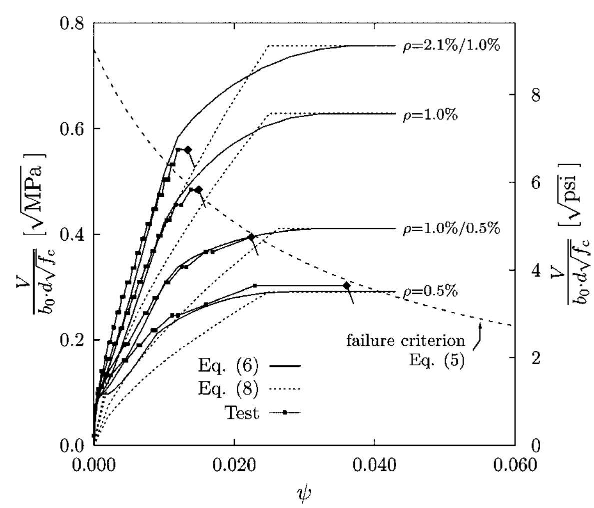

Fig. 12—Plots of load-rotation curves for tests by Kinnunen and Nylander[8] (refer to Fig. 8 for geometrical and mechanical parameters) and comparison to analytical laws of Eq. (6) and (8).

shown in Table 2 and plotted in Fig. 13 are the results from ACI 318-05[6] and Eurocode 2.[7] The results predicted by the proposed formulations are excellent, with an average ratio of effective to predicted load close to unity, and a very small coefficient of variation (COV) of 0.08, respectively, 0.09. Also remarkable is the minimum value of the ratio V_{test}/V_{th} given in Table 2. A ratio smaller than 1.0 means that the actual strength can be lower than predicted. It is 0.86 for both proposed formulations.

Tests in which failure occurred after reaching the flexural strength of the slab are also included in the results; in this case, setting the bending strength to its theoretical value (Eq. (7c)). This is why, in Fig. 13, a series of results are agglutinated along the inclined dotted line that delimits the bending failure mode.

The results given by the simplified Eq. (7) with a bilinear load-rotation relationship, not shown in the table, are very similar to those given by the complete solution of Eq. (6). This is not surprising because the considered test series include, above all, specimens with small or moderate slab thicknesses. By comparisons, the results of ACI 318-05[6] are generally much more conservative, which is to be expected from a design code, but with a much larger COV (0.22 with rounded critical section or 0.20 with a square-sized critical section), with the potential to actually lead to unsafe designs (the minimum value of the ratio V_{test}/V_{th} for the considered tests is 0.82). Furthermore, the ratio V_{test}/V_{th} strongly decreases for ACI 318-05[6] with increasing value of the effective depth of the slab (refer to tests by Hassanzadeh[22] and Hallgren[10] in Table 2 with d = 200 mm [7.87 in.] or Test PG-3 by Guandalini and Muttoni[13] with d = 456 mm [17.9 in.] in Fig. 9).

The results of Eurocode 2[7] are better, with a smaller average of the ratio, and also a smaller COV (average ratio of V_{test}/V_{th} equal to 1.14 and a COV of 0.12 with a minimum value of 0.86). It can be noted that Eurocode 2[7] limits the value of the factor affecting size effect for slabs with effective depths smaller than 200 mm (7.87 in.) to 2.0 (refer to Eq. (3)), which allows accounting for thickness tolerance for thin slabs. If this limit is not considered, the code equation shows better agreement to test results, with an average of 1.02 and a COV of 0.09, however, the minimum value of the ratio V_{test}/V_{th} decreases to 0.79.

Size effect

Size effect on punching shear strength was introduced initially in this paper by multiplying the slab rotation ψ by its thickness d in the formulation of Eq. (5). It is interesting to note that a slenderness effect (dependency on the ratio r_s/d) is present in the load-rotation relationship given by Eq. (8). Because the rotation according to this equation is inversely proportional to the slab thickness, if Eq. (8) is introduced into Eq. (5), the slab thickness d cancels on the right-hand side of the equation. Consequently, it follows that the factor for the reduction of the strength for size effect is not a function

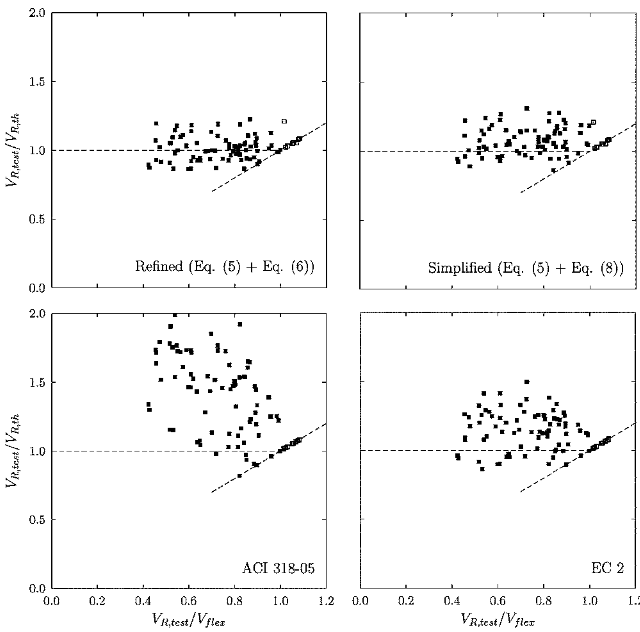

Fig. 13—Comparison of various formulations of ACI 318-05,[6] Eurocode 2,[7] and combination of Eq. (5) and (6) and of Eq. (5) and (8) with test results shown in Fig. 5 and Table 2.

Table 2—Comparison of results of test series with predicted strength of proposed approaches and of current design codes*; average, COV, and minimum value of ratio V_{test}/V_{th}

			Eq. (5) + Eq. (6)			Eq. (5) + Eq. (8)			ACI 318-05[6]			EC 2[7]		
Reference (year)	d, mm (in.)	No.	Average	COV	Minimum	Average	COV	Minimum	Average	COV	Minimum	Average	COV	Minimum
Elstner and Hognestad[18] (1956)	115 (4.52)	22	1.01	0.07	0.88	1.01	0.07	0.86	1.50	0.20	1.05	1.16	0.09	0.95
Kinnunen and Nylander[8] (1960)	122 (4.80)	12	1.02	0.09	0.86	1.08	0.08	0.96	1.45	0.18	1.03	1.14	0.13	0.90
Moe[19] (1961)	114 (4.48)	9	1.06	0.09	0.94	1.07	0.09	0.98	1.51	0.10	1.25	1.22	0.07	1.13
Schäfers[20] (1984)	113 to 170 (4.45 to 6.69)	4	1.02	0.08	0.93	1.06	0.10	0.94	1.41	0.14	1.16	1.25	0.05	1.19
Tolf[21] (1988)	98 to 200 (3.86 to 7.87)	8	0.98	0.10	0.87	1.06	0.10	0.92	1.33	0.21	0.98	1.11	0.14	0.94
Hassanzadeh[22] (1996)	200 (7.87)	3	0.97	0.09	0.87	1.04	0.08	0.95	1.10	0.06	1.03	1.03	0.14	0.86
Hallgren[10] (1996)	199 (7.83)	7	0.94	0.04	0.90	1.06	0.07	0.96	1.05	0.09	0.90	0.96	0.05	0.90
Ramdane[24] (1996)	98 (3.86)	12	1.07	0.08	0.94	1.16	0.08	1.03	1.43	0.23	0.91	1.22	0.12	1.00
Guandalini and Muttoni[13] (2004)	96 to 464 (3.78 to 18.2)	10	1.07	0.08	0.95	1.14	0.08	1.02	1.16	0.24	0.82	1.04	0.09	0.90
Σ		87	1.02	0.08	0.86	1.07	0.09	0.86	1.37	0.22	0.82	1.14	0.12	0.86

*Tests with different bending reinforcement ratios along orthogonal directions not included.
Note: COV = coefficient of variation.

of the slab thickness, but rather of the span, represented in Eq. (8) by the radius r_s of the isolated slab element.

CODE-LIKE FORMULATION

In 2003, Muttoni[17] proposed a similar relationship for the failure criterion for punching shear of flat slab systems assuming that $r_s = 0.22L$, where L is the span of the slab, and that the flexural capacity of the slab is $V_{flex} \cong 8m_{Rd}$ (where m_{Rd} is the flexural capacity of the slab in the column region reduced by the strength reduction factor). The resulting load-rotation relationship is thus

$$\psi = 0.33\frac{L}{d}\frac{f_y}{E_s}\left(\frac{V_d}{8m_{Rd}}\right)^{3/2} \tag{9}$$

where V_d is the factored shear force. Here again, the rotation is slenderness-dependent and thus it is inversely proportional to the thickness of the slab, with the consequence that the size effect factor of Eq. (5) is again a function of the span L of the slab and not of its thickness. Equation (9) is formulated for intermediate columns; for edge columns, the constant 8 is to be replaced by 4 and for corner columns by 2.

Equation (5), in a slightly rearranged form and to reach a target fractile of 5%, including a model factor to cover some irregularities in the spans and in disposition of the loading, has been introduced in the Swiss Code for structural concrete SIA 262[27] as

$$\frac{V_{Rd}}{b_0 d\sqrt{f_c'}} = \frac{2}{3\gamma_c}\frac{1}{1+20\frac{\psi d}{d_{g0}+d_g}} \text{ (SI units: N, mm)} \tag{10}$$

where γ_c is the partial safety factor of concrete ($\gamma_c = 1.5$) or

$$\frac{V_{Rd}}{b_0 d\sqrt{f_c'}} = \phi\frac{8}{1+20\frac{\psi d}{d_{g0}+d_g}} \text{ (U.S. customary units: psi, in.)}$$

where ϕ is the strength reduction factor for punching ($\phi = 0.75$).

Design approach

It is possible to combine Eq. (9) describing the load-deflection behavior of the slab element with the failure criterion of Eq. (10) into a single design formula. The exact punching strength (Point A in Fig. 14) is then obtained by setting V_{Rd} equal to V_d and iteratively solving the resulting equation. Requiring an iterative calculation even for the simplest cases, this formulation would not be very useful in practice. Instead, a simple design check can be performed calculating the slab rotation ψ_d corresponding to the factored shear force V_d using Eq. (9). From that value, the corresponding punching shear strength of the slab (Point B of Fig. 14) is found by applying Eq. (10). If the strength obtained from Eq. (10) is larger than the design load V_d, the design is safe and conservative. If, on the contrary, it is insufficient, the flexural reinforcement, the column size, or the slab thickness has to be increased.

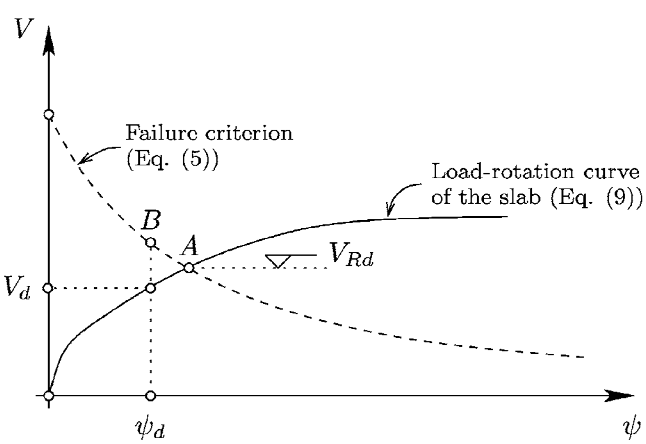

Fig. 14—Design procedure to check punching strength of slab.

Parametric study and comparison to test results

Figure 15 demonstrates the ability of the proposed formulation to investigate various aspects of the phenomenon of punching shear. As already known, an increase in the bending reinforcement leads to an increase in the punching shear capacity (Fig. 15(a)). This effect is not considered in the ACI 318-05[6] formulation, but is included in Eurocode 2[7] and the proposed formulation (where an increase in the bending reinforcement reduces the slab rotation ψ).

The effect of the size of the column relative to the thickness of the slab is illustrated in Fig. 15(b). This effect is considered by ACI, but only for large values of the ratio b_0/d. The proposed formulation, again, correctly describes this effect for the available test results, as does the formulation of Eurocode 2,[7] which handles it by working with a control perimeter located at $2d$ from the column face instead of $d/2$ for ACI and the present paper.

Figure 15(c) shows the effect of the effective slab thickness on the punching strength. The few available tests point toward a strong decrease for very thick slabs, which is correctly described by the proposed model and Eurocode 2[7] but ignored by ACI.

Concerning the effect of concrete strength on punching shear, Eurocode 2[7] and the proposed formulation give consistently good results, as shown in Fig. 15(d).

The effect of the type of steel used and of its yield stress f_y has been the object of only limited investigations, mostly by Moe.[19] This effect is not very pronounced, but a slight increase with increasing yield stress is predicted by the proposed formulation.

The span-depth ratio of the slab, represented by the ratio r_s/d for isolated slab elements also has an effect on the punching shear strength, according to the proposed formulation. This effect is considered neither by ACI 318-05[6] nor by Eurocode 2.[7] Further research should be devoted to investigate this aspect, as the punching strength of very slender slabs appears to be lower than expected, and no tests with significant thickness are currently available.

SUMMARY AND CONCLUSIONS

Design rules for punching shear present in design codes are generally based on experimental results performed on isolated slab elements representing the part of the slab close to the column. Most tests have been performed on relatively thin slabs, typically 0.1 to 0.2 m (4 to 8 in.). The test results are nonetheless commonly extrapolated to design flat slabs with a thickness typically 2 to 3 times larger, and even for foundation mats with thicknesses 10 to 20 times larger.

The present paper proposes a mechanical model based on the critical shear crack theory, explaining punching behavior

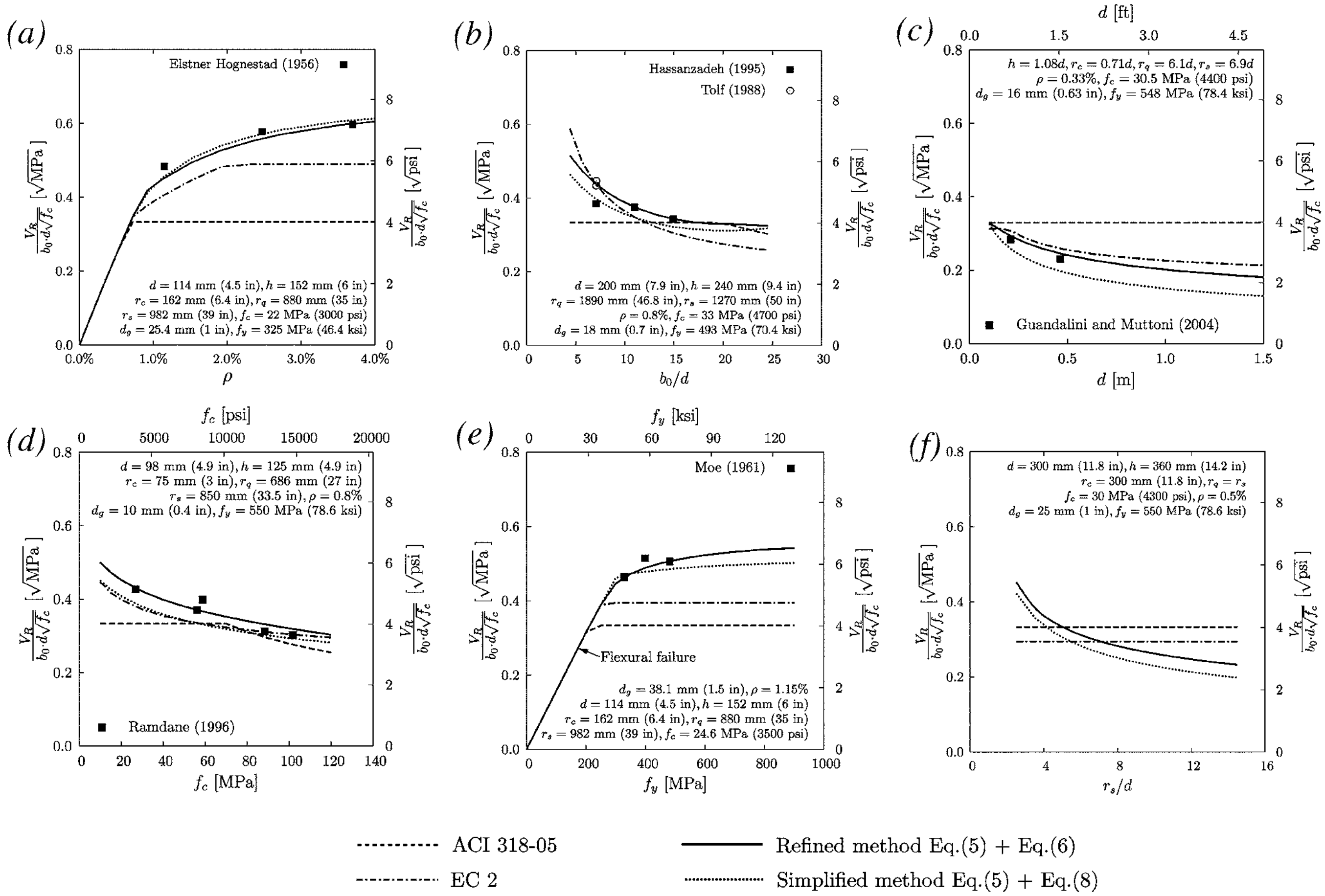

Fig. 15—Comparison of punching shear strength according to ACI 318-05,[6] Eurocode 2,[7] and the refined (Eq. (5) and (6)) and simplified (Eq. (5) and (8)) methods proposed in this paper with various test results showing influence of: (a) reinforcement ratio (tests by Elstner and Hognestad[18]); (b) punching shear perimeter (tests by Hassanzadeh[22] and Tolf[21]); (c) effective depth of slab (tests by Guandalini and Muttoni[13]); (d) concrete strength (tests by Ramdane[23]); (e) yield strength of steel (tests by Moe[19]); and (f) slenderness of slab.

of flat slabs without shear reinforcement and correctly accounting for size effect. A failure criterion is derived on its basis, which suitably describes the role of the many geometric and mechanical parameters involved in punching shear. The main conclusions of this paper are:

1. According to the proposed failure criterion, the punching strength is a function of the opening of a critical shear crack in the slab. Its influence is assumed to be proportional to the product of the slab rotation times the slab thickness and corrected by a factor to account for the maximum diameter of the aggregate;

2. This failure criterion simultaneously determines the punching load and the rotation capacity of the slab, and thus of its ductility;

3. The punching load can be determined by applying the failure criterion and a load-rotation relationship obtained from a nonlinear analysis of the slab in bending. For axisymmetric cases, an analytical formulation derived on the basis of a nonlinear moment-curvature diagram is given;

4. A simplified bilinear (elasto-plastic) moment-curvature relationship can also be applied to accurately estimate the punching load. The use of a more sophisticated moment-curvature relationship is only required for thick slabs with low reinforcement ratios, in which it is necessary to precisely account for the effects of the tensile strength of concrete and of tension stiffening;

5. A simplified analytical formulation of the load-rotation relationship, as it is used in the current Swiss design code for concrete structures, also gives a good estimate of the punching load;

6. The article proposes a method to calculate the punching strength as a function of the effective depth of the slab, the size of the column, the flexural reinforcement ratio, the yield strength of the reinforcing steel, the concrete strength, the maximum aggregate size, and the span-depth ratio of the slab. This method gives very good results when compared with a series of 87 test results, with a COV of the ratio V_{test}/V_{th} of 8%;

7. Size effect on the punching shear strength is accounted in the failure criterion of the critical shear crack theory. This effect, in combination with the slenderness effect on the load-rotation relationship proposed in this paper, can be formulated as a function of the span of the slab;

8. ACI 318-05[6] does not only exhibit a very large COV when compared with test results (22%), but it does not include important effects, which leads to unsafe designs in particular for thick and/or slender slabs with low reinforcement ratios;

9. Eurocode 2[7] has a better COV when compared with test results (12%), but it also can predict unconservative values for slender slabs;

10. Even if tests on thin slabs have exhibited some level of ductility for low reinforcement ratios, the behavior is quite brittle for thicker slabs; and

11. For thick slabs, the only solution to reach a satisfactory level of ductility is to place punching shear reinforcement.

ACKNOWLEDGMENTS

The work presented in this paper was funded by the Association of the Swiss Cement Industry (cemsuisse) and by the Swisscode project of the Swiss Society of Engineers and Architects (SIA). The author is appreciative of the support received.

REFERENCES

1. Gasparini, D. A., "Contributions of C. A. P. Turner to Development of Reinforced Concrete Flat Slabs 1905-1909," *Journal of Structural Engineering*, ASCE, V. 128, No. 10, 2002, pp. 1243-1252.

2. Fürst, A., and Marti, P., "Robert Maillart's Design Approach for Flat Slabs," *Journal of Structural Engineering*, ASCE, V. 123, No. 8, 1997, pp. 1102-1110.

3. Silfwerbrand, J., and Hassanzadeh, G., eds., "International Workshop on Punching Shear Capacity of RC Slabs," Royal Institute of Technology, Stockholm, Sweden, 2000, 527 pp.

4. FIB, "Punching of Structural Concrete Slabs," *fib Bulletin* 12, Lausanne, Switzerland, 2001, 307 pp.

5. Polak, M. A., ed., *Punching Shear in Reinforced Concrete Slabs*, SP-232, American Concrete Institute, Farmington Hills, MI, 2005, 302 pp.

6. ACI Committee 318, "Building Code Requirements for Structural Concrete (ACI 318-05) and Commentary (318R-05)," American Concrete Institute, Farmington Hills, MI, 2005, 430 pp.

7. Eurocode 2, "Design of Concrete Structures—Part 1-1: General Rules and Rules for Buildings," CEN, EN 1992-1-1, Brussels, Belgium, 2004, 225 pp.

8. Kinnunen, S., and Nylander, H., "Punching of Concrete Slabs Without Shear Reinforcement," *Transactions of the Royal Institute of Technology*, No. 158, Stockholm, Sweden, 1960, 112 pp.

9. Alexander, S. D. B., and Hawkins, N. M., *A Design Perspective on Punching Shear*, SP-232, M. A. Polak, ed., American Concrete Institute, Farmington Hills, MI, 2005, pp. 97-108.

10. Hallgren, M., "Punching Shear Capacity of Reinforced High Strength Concrete Slabs," doctoral thesis, Royal Institute of Technology, Stockholm, Sweden, 1996, 206 pp.

11. Broms, C. E., *Concrete Flat Slabs and Footings: Design Method for Punching and Detailing for Ductility*, Royal Institute of Technology, Stockholm, Sweden, 2006, 114 pp.

12. Muttoni, A., and Schwartz, J., "Behaviour of Beams and Punching in Slabs without Shear Reinforcement," IABSE Colloquium, V. 62, Zurich, Switzerland, 1991, pp. 703-708.

13. Guandalini, S., and Muttoni, A., "Symmetric Punching Tests on Reinforced Concrete Slabs without Shear Reinforcement," Test report, EPFL, Lausanne, Switzerland, 2004, 78 pp. (in French)

14. Bollinger, K., "Load-Carrying Behaviour and Reinforcement of Axisymmetrically Loaded Reinforced Concrete Plates," doctoral thesis, Abteilung Bauwesen der Universität Dortmund, Dortmund, Germany, 1985, 262 pp. (in German)

15. Walraven, J. C., "Fundamental Analysis of Aggregate Interlock," *Journal of Structural Engineering*, ASCE, V. 107, No. 11, 1981, pp. 2245-2270.

16. Vecchio, F. J., and Collins, M. P., "The Modified Compression-Field Theory for Reinforced Concrete Elements Subjected to Shear," ACI JOURNAL, *Proceedings* V. 83, No. 2, Mar.-Apr. 1986, pp. 219-231.

17. Muttoni, A., "Shear and Punching Strength of Slabs without Shear Reinforcement," *Beton-und Stahlbetonbau*, V. 98, No. 2, Berlin, Germany, 2003, pp. 74-84. (in German)

18. Elstner, R. C., and Hognestad, E., "Shearing Strength of Reinforced Concrete Slabs," ACI JOURNAL, *Proceedings* V. 53, No. 2, Feb. 1956, pp. 29-58.

19. Moe, J., "Shearing Strength of Reinforced Concrete Slabs and Footings under Concentrated Loads," V. D47, PCA, IL, 1961, 135 pp.

20. Schäfers, U., "Construction, Dimensioning and Safety with Respect to Punching Shear of Reinforced Concrete Flat Plates in the Vicinity of Internal Columns," *Deutscher Ausschuss für Stahlbeton*, No. 357, Berlin, Germany, 1984, 83 pp. (in German)

21. Tolf, P., "Influence of the Slab Thickness on the Strength of Concrete Slabs at Punching: Tests with Circular Slabs," No. 146, Royal Institute of Technology, Stockholm, Sweden, 1988, 64 pp. (in Swedish)

22. Hassanzadeh, G., "Strengthening of Bridge Slabs with Respect to Punching: Test Results," *Report* 41, Royal Institute of Technology, Stockholm, Sweden, 1996, 134 pp. (in Swedish)

23. Ramdane, K.-E., "Punching Shear of High Performance Concrete Slabs," *Utilization of High-Strength/High Performance Concrete*, Proceedings of the Fourth International Symposium, V. 3, Paris, France, 1996, pp. 1015-1026.

24. Nylander, H., and Sundquist, H., "Punching of Bridge Slabs with Non-Prestressed Reinforcement on Columns," No. 104, Royal Institute of Technology, Stockholm, Sweden, 1972, 64 pp. (in Swedish)

25. Kinnunen, S.; Nylander, H.; and Tolf, P., "Influence of the Slab Thickness on the Strength of Concrete Slabs at Punching: Tests with Rectangular Slabs," *Test Report*, Royal Institute of Technology, No. 137, Stockholm, Sweden, 1980, 73 pp. (in Swedish)

26. Guandalini, S., "Symmetric Punching in R/C Slabs," doctoral thesis, No. 3380, EPFL, Lausanne, Switzerland, 2005, 289 pp. (in French)

27. SIA, "262 Code for Concrete Structures," Swiss Society of Engineers and Architects, Zurich, Switzerland, 2003, 94 pp.

APPENDIX 1

In this appendix, a load-rotation relationship for an isolated slab element is derived based on the assumption that the deflected shape of the isolated slab element is conical outside the critical shear crack. The curvature in tangential direction (Fig. 6f) is thus:

$$\chi_t = -\frac{\psi}{r} \quad \text{for } r > r_0 \tag{11}$$

Inside the critical shear crack, it may be assumed that the curvatures in both directions are constant and equal (Figs 6d,f), so that the deflected shape is spherical :

$$\chi_r = \chi_t = -\frac{\psi}{r_0} \quad \text{for } r \le r_0 \tag{12}$$

With these curvatures, the internal forces described in Figs 6b,c can be calculated according to the quadrilinear moment-curvature relationship shown in Fig. 7. This relationship is characterized by the stiffnesses EI_0 before and EI_1 after cracking, the cracking moment m_{cr} , the moment capacity m_R and the tension stiffening effect χ_{TS}. Neglecting the effect of reinforcement before cracking, these terms can be obtained as:

$$m_{cr} = \frac{f_{ct} \cdot h^2}{6} \tag{13}$$

$$EI_0 = \frac{E_c \cdot h^3}{12} \tag{14}$$

$$-\chi_{cr} = \frac{m_{cr}}{EI_0} = \frac{2 \cdot f_{ct}}{h \cdot E_c} \tag{15}$$

Assuming a linear-elastic behaviour of steel and concrete after cracking, it follows:

$$EI_1 = \rho \cdot \beta \cdot E_s \cdot d^3 \cdot \left(1 - \frac{c}{d}\right) \cdot \left(1 - \frac{c}{3d}\right) \tag{16}$$

where c is the depth of the compression zone:

$$c = \rho \cdot \beta \cdot \frac{E_s}{E_c} \cdot d \cdot \left(\sqrt{1 + \frac{2 \cdot E_c}{\rho \cdot \beta \cdot E_s}} - 1\right) \tag{17}$$

and β is an efficiency factor that accounts for the orthogonal layout of the reinforcement and the reduction in the ratio between the torsion and bending stiffness of the slab after cracking. It should be noted that this factor affects the stiffness of the member but not the flexural strength of the member. While the developments above were made for a layout with a polar symmetry (reinforcement placed in radial and tangential directions), reinforcement is usually placed orthogonally in the slab. For these cases, a good agreement to test data is obtained assuming $\beta = 0.6$.

Assuming a perfectly plastic behaviour of the reinforcement after yielding, a rectangular stress block for concrete in the compression zone and neglecting compression reinforcement, the moment capacity m_R of the section is then:

$$m_R = \rho \cdot f_y \cdot d^2 \cdot \left(1 - \frac{\rho \cdot f_y}{2 \cdot f_c}\right) \tag{18}$$

The decrease in curvature caused by tension stiffening can be approximated by the constant contribution χ_{TS}:

$$\chi_{TS} = \frac{f_{ct}}{\rho \cdot \beta \cdot E_s} \cdot \frac{1}{6 \cdot h} \tag{19}$$

which corresponds approximately to $0.5 \cdot m_{cr} / EI_1$.

The curvatures χ_1 at the beginning of the stabilized cracked regime and χ_y at yielding are thus:

$$-\chi_1 = \frac{m_{cr}}{EI_1} - \chi_{TS} \tag{20}$$

and

$$-\chi_y = \frac{m_R}{EI_1} - \chi_{TS} \tag{21}$$

The four segments of the assumed moment-curvature relationship correspond to the four regions of the slab shown in Figs 6f,g. The radii delimiting these zones may be determined by substituting Eqs (15), (20) and (21) into Eq. (11), as follows:

Zone within which the reinforcement is yielding, plastic radius r_y:

$$r_y = -\frac{\psi}{\chi_y} = \frac{\psi}{\dfrac{m_R}{EI_1} - \chi_{TS}} \le r_s \tag{22}$$

Zone in which cracking is stabilized, radius r_1:

$$r_1 = -\frac{\psi}{\chi_1} = \frac{\psi}{\dfrac{m_{cr}}{EI_1} - \chi_{TS}} \le r_s \tag{23}$$

and zone up to which the concrete is cracked, cracking radius r_{cr} :

$$r_{cr} = -\frac{\psi}{\chi_{cr}} = \frac{\psi \cdot EI_0}{m_{cr}} \le r_s \tag{24}$$

The equilibrium equation of the slab portion shown in Fig. 6c is:

$$V \cdot \frac{\Delta\varphi}{2\pi} \cdot \left(r_q - r_c\right) = -m_r \cdot \Delta\varphi \cdot r_0 - \Delta\varphi \cdot \int_{r_0}^{r_s} m_\varphi \cdot dr \tag{25}$$

where m_r is the radial moment at $r = r_0$ calculated according to Fig. 7 with the curvature given by Eq. (12). It follows that:

$$V = \frac{2\pi}{r_q - r_c} \cdot \begin{pmatrix} -m_r \cdot r_0 + m_R \cdot \langle r_y - r_0 \rangle + EI_1 \cdot \psi \cdot \langle \ln(r_1) - \ln(r_y) \rangle + \\ EI_1 \cdot \chi_{TS} \cdot \langle r_1 - r_y \rangle + m_{cr} \cdot \langle r_{cr} - r_1 \rangle + EI_0 \cdot \psi \cdot \langle \ln(r_s) - \ln(r_{cr}) \rangle \end{pmatrix} \tag{6}$$

where the operator $\langle x \rangle$ is x for $x \ge 0$ and 0 for $x < 0$

APPENDIX 2

The following symbols are used in the paper:

E_c	=	modulus of elasticity of concrete (assumed $E_c = 10'000 \cdot f_c^{1/3}$ [MPa], $E_c = 276'000 \cdot f_c^{1/3}$ [psi])
E_s	=	modulus of elasticity of reinforcement
EI_0	=	flexural stiffness before cracking
EI_1	=	tangential flexural stiffness after cracking
L	=	main span of a slab system

V = shear force

V_d = factored shear force

V_{flex} = shear force associated with flexural capacity of the slab

V_R = nominal punching shear strength

V_{Rd} = design punching shear strength

V_{test} = experimental punching shear strength

V_{th} = theoretical punching shear strength

b_0 = perimeter of the critical section for punching shear

b_c = side length of a square column

b_s = side length of a square isolated slab element

c = distance from extreme compression fibre to neutral axis

d = distance from extreme compression fibre to the centroid of the longitudinal tensile reinforcement

d_b = diameter of a reinforcement bar

d_g = maximum diameter of the aggregate

d_{g0} = reference aggregate size (16 mm (0.63 in))

f_c = average compressive strength of concrete (cylinder)

f'_c = specified compressive strength of concrete (cylinder)

f_{ct} = tensile strength of concrete (assumed $f_{ct} = 0.3 \cdot f_c^{2/3}$ [MPa], $f_{ct} = 1.6 \cdot f_c^{2/3}$ [psi])

f_y = yield strength of reinforcement

h = slab thickness

m_{cr} = cracking moment per unit width

m_r = radial moment per unit width

m_t = tangential moment per unit width

m_R = nominal moment capacity per unit width

m_{Rd} = design moment capacity per unit width

r	=	radius
r_0	=	radius of the critical shear crack
r_1	=	radius of the zone in which cracking is stabilized
r_c	=	radius of a circular column
r_{cr}	=	radius of cracked zone
r_q	=	radius of the load introduction at the perimeter
r_s	=	radius of circular isolated slab element
r_y	=	radius of yielded zone
$\Delta\varphi$	=	angle of a slab sector
β	=	efficiency factor of the bending reinforcement for stiffness calculation
γ_c	=	partial safety factor for concrete (according to European practice, $\gamma_c = 1.5$)
ρ	=	reinforcement ratio
ϕ	=	strength reduction factor (according to North-American practice, $\phi = 0.75$ for shear)
χ_1	=	curvature in stabilized cracking
χ_{cr}	=	curvature at cracking
χ_r	=	curvature in radial direction
χ_t	=	curvature in tangential direction
χ_y	=	yielding curvature
χ_{TS}	=	decrease in curvature due to tension stiffening
ψ	=	rotation of slab outside the column region
ψ_d	=	rotation of slab outside the column region due to factored shear force V_d
ξ	=	size effect coefficient in Eurocode 2[7]

Disc. 105-S37/From the July-August 2008 *ACI Structural Journal*, p. 395 and p. 405

Design of Deep Beams Using Strut-and-Tie Models—Part I: Evaluating U.S. Provisions and **Part II: Design Recommendations.** Papers by Michael D. Brown and Oguzhan Bayrak

Discussion by Dipak Kumar Sahoo, Bhupinder Singh, and Pradeep Bhargava

Research Scholar, Department of Civil Engineering, Indian Institute of Technology Roorkee, Roorkee, India; Assistant Professor, Department of Civil Engineering, Indian Institute of Technology Roorkee; Professor, Department of Civil Engineering, Indian Institute of Technology Roorkee

The authors are complimented for the exhaustive compilation and meticulous evaluation of a large database of 596 reinforced concrete beams with *a*/*d* ratios less than 2 to identify the unconservatism in the strut-and-tie model (STM) provisions of ACI 318-05 and the AASHTO LRFD. Recently, Yang and Ashour (2008) analyzed a large shear database, part of which is also used by the authors, and observed similar unconservatism in the STM provisions of the ACI 318-05 and the Eurocode 2 (2004) as well, with these provisions being even more unsafe, particularly for continuous deep beams. The discussers would like to draw the authors' attention to two points:

1. With reference to the findings of Part I, it may be noted that the cylinder compressive strengths of concrete used in the 596 beams of the database fall in a wide range—28 to 83 MPa (4000 to 12,000 psi)—whereas the applicability of the STM provisions of ACI 318-05, Appendix A, is limited to concrete with compressive strengths up to 41 MPa (6000 psi). The literature suggests that the strut efficiency factor decreases with an increase in the concrete compressive strength and, therefore, it should be expected that the higher-strength concrete beams will be unsafe when evaluated using the ACI 318-05 provisions; and

2. With reference to Fig. 1 of Part II, the authors have suggested a correlation of the following form between the strut efficiency factor ν and the two important influencing parameters: the shear span-to-effective depth ratio (*a*/*d*) and the concrete compressive strength f_c'.

$$\nu = k_0 (a/d)^{-1} (\sqrt{f_c'})^{-1} \tag{A}$$

The strut efficiency factor is known to decrease with an increase in the concrete compressive strength f_c'. Because the strut efficiency is related to the splitting tensile strength of concrete, a parameter linearly linked to $\sqrt{f_c'}$, the authors are fully justified in correlating ν with $\sqrt{f_c'}$. However, the discussers are not clear why the authors have chosen a power function to correlate ν with the *a*/*d*, which is simply $\cot\theta$, with θ being the angle of inclination of the strut with the horizontal.

The composite correlation pattern followed by the authors in Eq. (A) can be expressed as two independent power functions indicated in the following

$$\nu \alpha \frac{1}{(a/d)^{k_1}} \tag{B}$$

$$\nu \alpha \frac{1}{(f_c')^{k_2}} \tag{C}$$

where k_1 and k_2 are two independent exponents that can be evaluated by suitably grouping the database considering one parameter at a time while keeping the other parameter constant. Finally, combining Eq. (B) and (C), the composite model relating the strut efficiency factor ν to the *a*/*d* and f_c' will become

$$\nu = k_0 (a/d)^{-k_1} (f_c')^{-k_2} \tag{D}$$

where k_0 is a constant coefficient that can also be evaluated from the database.

The discussers feel that unless the values of both k_1 and k_2 (evaluated using the database as discussed) are close enough to unity, two independent exponents may be preferred.

REFERENCES

EN 1992-1-1:2004, 2004, "Eurocode 2: Design of Concrete Structures—Part 1-1: General Rules and Rules for Buildings," British Standards Institution, London, UK., 225 pp.

Yang, K.-H., and Ashour, A. F., 2008, "Code Modeling of Reinforced-Concrete Deep Beams," *Magazine of Concrete Research*, V. 60, No. 6, pp. 441-454.

AUTHORS' CLOSURE

The authors would like to thank the discussers for their interest, and hope these comments resolve the outstanding issues related to the papers.

The discussers present two comments related to the two-part paper. The first comment relates to the limitation of 6000 psi (41 MPa) in Appendix A of ACI 318. This limitation applies only to Section A.3.3.1 and no other provisions within Appendix A. Additionally, when examining the effects of concrete compressive strength within the database of experimental results, the authors did not find a significant difference between test results of various strengths of concrete. This result may be due to the relatively limited data stemming from tests with high-strength concrete.

The second point raised by the discussers relates to the choice of the exponent in the proposed equations. The two parameters (*a*/*d* and $\sqrt{f_c'}$) were evaluated independently though the course of developing the proposed equations. In both cases, the values of the exponents were very close to 1.0. Figure 1 was intended to illustrate that result with the value of the exponent on the product of the two parameters equal to 0.97.

Disc. 105-S37/From the July-August 2008 *ACI Structural Journal*, p. 395

Design of Deep Beams Using Strut-and-Tie Models—Part I: Evaluating U.S. Provisions. Paper by Michael D. Brown and Oguzhan Bayrak

Discussion by Andor Windisch

ACI Member, PhD, Karlsfeld, Germany

The historical remembrance is sometimes incorrect: the truss mechanism where the stirrups act in pure tension was proposed by Hennebique in his patent. Reporting on this patent, Ritter[1] was in doubt about this. He proposed to place the stirrups along the tensile trajectories 45 degrees inclined to the supports.

CURRENT U.S. CODE PROVISIONS

The authors are to be complimented for their concise summary of the current code provisions for the use of strut-and-tie modeling. In Fig. 1 and Table 1, the strut efficiency factors are given:

- In the case of a strut with a uniform cross section over its length, $\beta = 1.0$.
- This is the case when (using the legend of Fig. 1) $b = L$ but also when $L = b$, that is, when the strut with $b = h$ is loaded on its full width.

The following comments arise:

- According to the theory of plasticity, the failure load does not decrease if the cross section is increased with load-bearing material.
- Being so, why is the effective compression strength f_{ce} less if $L < b$, that is, the total loading is much less?
- In the Eurocode 2 (2004), the minimum reinforcement according to Eq. (2) (with $\alpha = 90$ degrees) is obligatory in all reinforced concrete structures, even in the case of struts with an assumed uniform cross section over their length.

The sudden failure of the specimen during the split cylinder test is mentioned as the formidable example of the jeopardizing effect of induced tension. Nevertheless, one should calculate the compressive stress along the line load on the cylinder and compare it to the effective compressive strength according to Table 1. Huge differences exist!

The crack shown in Fig. 3 of the paper has nothing to do with the dispersion of the compressive force in the bottle-shaped strut, that is, tensile stresses induced by the associated equilibrium, and does not reduce the load-bearing capacity of this strut.

Looking at the struts in Fig. 5, why is the strut in the compression zone not forming a bulge, at least downwards? Conclusion: the bottle-shaped strut is a useless component of a questionable model in fashion.

Why is the strut-and-tie model, which is so easy to be applied, questionable? It is dangerous, as it may give the impression that having a closed system of dashed and continuous lines (struts and ties) and maybe some concrete efficiency factors, will make the structural member safe. For example, deep beams with shear span-depth ratios of approximately 1 or less, with flexural reinforcement determined according to the strut-and-tie models shown in Fig. 4 and the truss models shown in Fig. 5 would fail in flexure.

With reference to the modified compression field theory (MCFT)-based usable compressive stress in the strut, it was shown (Windisch 2000) that the failure of most reinforced concrete panels (all of which were loaded by deformation control) was caused by the yielding of the weaker char of reinforcement in the panel. Therefore, Eq. (3) and (4) can not be related to allowable concrete stresses. The authors' reservation concerning the calculation of the average concrete strain during the design process is more than justified.

DATABASE OF EXPERIMENTAL RESULTS

Irrespective of the sense of database evaluations, the data should be split with reference to the type of reinforcement: earlier tests beams (for example, contained mild steel round bars) having an average yield stress of 46,000 psi (317 N/mm^2).[35] These results shall be treated separately. In many of the specimens, the shear failure occurred after the flexural reinforcement yielded, that is, the flexural capacity was exhausted; hence, these specimens should also be excluded.

STRAIN ENERGY IN STRUT-AND-TIE MODELS

The discusser wondered about the possibility of the highly subjective choice of models. The recommendation[11] that the model with the least strain energy is likely to be the most appropriate is not verified. The authors are to be complimented that they pointed it out as well. If this recommendation is true, then the application of refined strut-and-tie models—as suggested in SP-208[17]—could not be possible.

The two-panel model in Fig. 5(b) was chosen for panels with vertical shear reinforcement. The corresponding vertical tie turned the strut. Nevertheless, neither the trajectories nor the crack pattern of the panel are influenced by the vertical shear reinforcement. It would have been more realistic to make use of the one-panel model, increasing the efficiency factor of the strut in relationship to the rate of reinforcement.

Concerning the combined model, the following questions arise: How does the efficiency of the inclined strut of the one-panel truss interfere with the tension in the vertical tie of the two-panel truss? Does it increase it or reduce it?

SUMMARY AND CONCLUSIONS

As mentioned previously, the control of the load-bearing capacity of the single direct strut between the load point and the reaction may result in specimens that fail in flexure. It would be interesting to find out which type of failures occurred at those beams that showed efficiency factors less than the nominal values. Do the strut efficiency factors remain valid in the case of deep beams with uniformly distributed loading on their top or when the concentrated load acts on the bottom edge of the beam?

REFERENCES

EN 1992-1-1, 2004, "Eurocode 2: Design of Concrete Structures—Part 1-1: General Rules and Rules for Buildings," Brussels, Belgium, 225 pp.

Windisch, A., 2000, "On the Design of Two-Way Reinforcements in R/C," Studi e ricerche, Scuola di specializzazione in Costruzioni in C. A. Fratelli Pesenti, Politecnico di Milano, V. 21, pp. 283-302.

Disc. 105-S38/From the July-August 2008 *ACI Structural Journal*, p. 405

Design of Deep Beams Using Strut-and-Tie Models—Part II: Design Recommendations. Paper by Michael D. Brown and Oguzhan Bayrak

Discussion by Andor Windisch

ACI Member, PhD, Karlsfeld, Germany

DEVELOPMENT OF EFFICIENCY FACTOR EQUATIONS

Analysis of database

It can be treated as a deficiency of the new expression for the efficiency factor that the square root of the compressive strength was taken as a parameter. This could give the impression that the concrete tensile strength has some fundamental influence on the shear strength of strut efficiency, which physically can not be the case. It might be that an improved definition of the effective shear span (taking into account the effective lengths of the plates at support and loading) could have been found to decrease the scatter.

Reinforcement in bottle-shaped strut

According to the authors, the reason for the reinforcement in bottle-shaped struts is to carry the transverse splitting force after the formation of the splitting crack along the axis of the strut. As already discussed with regard to Part I, the bottle-shaped strut is a questionable formation. Moreover, until now, any reinforcement beyond the minimum reinforcement according to ACI 318-05 should be included into the truss as a tie, which rearranges the truss configuration. Suddenly, a calculated amount of reinforcement is hidden behind a dashed line (strut). How can a dashed line be perceived as an ordinary strut or one with reinforcement, which must be dimensioned? Why does a strut that models the compression zone not split? In general, a strut does not fail through splitting but rather along a sliding surface. This develops mostly at the end of a flexural-shear or shear crack. The flexural-shear or shear crack borders the strut, but does not split it.

Node geometry

The authors are completely correct: whether the node is hydrostatic or not is a rather irrelevant question. When the web has the same width as the bottom flange at the support, then only two tasks must be solved by the engineer: proper size of the bearing plate (with some local zone reinforcement) and the proper anchorage of the longitudinal reinforcement. Hence any further theorization of the node problem might be impressive, but remains useless.

COMPARISON OF STRUT-AND-TIE MODEL PROVISIONS AND SUMMARY

The histograms (Fig. 10 through 12) of the ultimate strength to nominal strength ratio with the high rate of over-dimensioned specimens permits a single conclusion only: even if the strut-and-tie model would be a proper model, the strength of the inclined struts is certainly not the governing factor for safe structures. The authors are strongly encouraged to continue their activity to detect all inconsistencies of the strut-and-tie models.

AUTHORS' CLOSURE

The discusser presents many questions related to the use of bottle-shaped struts. In general, the authors are in agreement with the discusser's comments. The splitting crack that forms in a bottle-shaped strut is a serviceability concern in most cases rather than a strength concern. After the splitting crack forms, the tensile stresses in concrete along the crack vanish and the state of stress more closely resembles uniaxial compression. As Cross (1952) noted, however, strength is not the only concern. The presence of transverse reinforcement in a bottle-shaped strut will help to reduce crack widths at service loads, which improves durability provided that service level loads do not result in yielding of these bars. Given that these horizontal bars are likely present in most cases, it is prudent to consider them in the truss model. The authors agree with the discusser's comments regarding strut without transverse reinforcement: they should be avoided as stated in Part I.

The authors disagree with the discusser's suggestion that specimens in which the longitudinal reinforcement reached yield before shear failure occurred should be excluded from the database. Rather, these are the primary specimens that should be examined. Current ACI 318 Code provisions are based on some level of ductility within a properly designed structure. The use of different strength reduction factors for the various failure modes is evidence of this fact. Furthermore, the assumption of a fully plastic structure undergoing plastic deformations, consistent with strut-and-tie modeling, suggests that the reinforcement has yielded before failure occurs. A ductile failure mode, such as yielding of the reinforcement, is preferable to a brittle one, such as crushing of a strut.

The authors' examination of strain energy in the strut-and-tie models was not refined to the degree necessary to answer the discusser's questions. This evaluation of strain energy, as stated in the paper, was a simplistic attempt to examine the concept of minimum strain energy in various models. To that end, limited though it may have been, the authors believe the attempt was successful for the stated objective.

The authors' classified specimens based on the various failure types by using definitions developed by Kani et al.[28] (in Part I). No strong correlation between Kani et al.'s failure types and efficiency factor was found. The specimens studied in this database, however, were confined to two of Kani et al.'s four failure types. Perhaps this classification may have been too crude to yield meaningful results.

In regard to the discusser's question about deep beams with uniform loads applied on the top of a beam or a concentrated load applied near the bottom of a beam, the authors can provide some insight. Based on previously published research by the authors (Brown and Bayrak 2006; Brown et al. 2006), it would be expected that the failure loads of specimens subjected to distributed loads on their top surface would be higher than the failure loads predicted using the equations presented in these papers. As for specimens subjected to concentrated loads near their bottom surface, the authors would expect the failure loads predicted with the proposed equations could overestimate the shear strength. This overestimation would be due to the tensile stresses induced in the web of such a member. This particular question, however, has not been studied by the authors, and our supposition that specimens loaded near their bottom surface should be taken for what it is: speculation based on review of limited experimental research related to such structures.

REFERENCES

Brown, M. D., and Bayrak, O., 2007, "Investigation of Deep Beams with Various Load Configurations," *ACI Structural Journal*, V. 104, No. 5, Sept.-Oct., pp. 611-620.

Brown, M. D.; Bayrak, O.; and Jirsa, J. O., 2006, "Design for Shear Based on Loading Conditions," *ACI Structural Journal*, V. 103, No. 4, July-Aug., pp. 541-550.

Cross, H., 1952, *Engineers and Ivory Towers*, McGraw-Hill, New York, 142 pp.

Disc. 105-S42/From the July-August 2008 *ACI Structural Journal*, p. 440

Punching Shear Strength of Reinforced Concrete Slabs without Transverse Reinforcement. Paper by Aurelio Muttoni

Discussion by Andor Windisch

ACI member, PhD, Karlsfeld, Germany

The author is to be complimented for his new failure criterion for punching shear based on the critical shear crack theory. The failure procedure is explained[12] as follows: "the shear strength is reduced by the presence of a critical shear crack that propagates through the slab into the inclined compression strut carrying the shear force to the column."

Regarding Fig. 2, this explanation shall be complemented as follows: at the critical shear crack shown in Fig. 2(a), the continuous thick line consists of (at least) two different sections—the upper part is a typical flexural-shear crack and the lower part is a sliding surface across the compression zone of the slab around the column, that is, this part cannot be considered an "ordinary" crack. The theoretical strut depicted in Fig. 2(b) cannot exist as described. It does not develop around the critical shear crack, nor develops the critical crack across the strut. The source of the inclined compressive force in this strut, as shown in Fig. 2(b), is not clear either. How does it develop on the top of the slab? The discusser would like to assume that the author had similar doubts. The elbowed-shaped strut in Fig. 2(c) confirms this feeling. The sliding surface part of the critical shear crack crosses the node where both struts join. The truss model with the elbow-shaped strut shown in Fig. 2(c) is completely irrelevant (as is the entire strut-and-tie model). How would a shifting of the loading, for example toward the column, influence the truss? And concerning the load-bearing capacity of the triple lines, the ties that should had been of concrete: who cares? The strut-and-tie model shows its limits very clearly.

The discusser means that the source of the punching shear strength of slabs without transverse reinforcement is the shear load-bearing capacity of the compression zone.[28] The inclined or curved compression strut has no function at all. The contributions of shear friction and dowel action can be neglected, too. (The size effect originates from the limited extent of the process zone in fracture mechanics and must be taken into account.)

The shear strength formulas in the different codes, that is, Eq. (1), (2), and (4), referring to the slab depth d and the arbitrary control perimeter, smear the different contributions. The smeared, mechanically inconsistent material characteristic is than approximated with $f_c'^{1/2}$ or $f_c'^{1/3}$, which have no real physical meaning; they are relatively close to the calculated figures only.

The author's interesting new failure criterion based on the rotation of the slab must be opposed due to the two load-rotation curves shown in Fig. 3(a). The detrimental effect of the supplementary reinforcing ring d_b12 (one No. 4) cannot be predicted by the rotation. Menétrey[29] found similar jeopardizing influence of reinforcing rings in his tests.

The author is correct: the punching strength is a function of the opening of a critical shear crack in the slab. Nevertheless, the position of this crack can not be predicted through the slab rotation, hence ψ can not be considered as an independent variable of the phenomenon.

The paper gives very valuable impacts for looking for a mechanically sound model on punching shear strength.

REFERENCES

28. Windisch, A., "Towards a Consistent Design Model for Punching Shear Capacity," International Workshop on Punching Shear Capacity of RC Slabs, Royal Institute of Technology, Stockholm, Sweden, 2000, pp. 293-301.

29. Menétrey, P., "Relationship between Flexural and Punching Failure," *ACI Structural Journal*, V. 95, No. 4, July-Aug. 1998, pp. 412-419.

Disc. 105-S42/From the July-August 2008 *ACI Structural Journal*, p. 440

Punching Shear Strength of Reinforced Concrete Slabs without Transverse Reinforcement. Paper by Aurelio Muttoni

Discussion by N. Subramanian

ACI member, PhD, Consulting Structural Engineer, Gaithersburg, MD

The author has to be appreciated for developing a comprehensive analytical model for predicting the punching shear strength of reinforced concrete slabs without transverse reinforcement. It is also interesting to note that the author has developed failure criteria based on a given critical rotation of the slab, and that a similar proposal has been included in the Swedish standards.

However, the equation for calculating m_{Rd} (the flexural capacity of the slab in the column region reduced by the strength reduction factor) used in Eq. (9) is not given. Only when m_{Rd} is evaluated can the load-rotation relationship and the punching shear strength be calculated. Hence, the author is requested to give the equation for the same.

In this connection, the discusser wishes to note another comprehensive analytical model developed by Theodorakopoulos and Swamy[30] to predict the ultimate punching shear strength of slab-column connections. This model is also based on the physical behavior of the connections and is applicable to both lightweight and normalweight concrete. It also incorporates several variables that affect the punching shear strength of flat slabs including the concrete strength, tension steel ratio, compression reinforcement, and loaded area. It was compared with 60 reported tests in literature and found to agree with them with reasonable accuracy. The discusser requests that the author compare the results of his analytical model with their results, and show the significant advantage of using his model. The discusser is unable to do so due to the unavailability of the equation for m_{Rd} in Eq. (9).

Theodorakopoulos and Swamy[31] recently extended the aforementioned theory for predicting the punching shear strength of FRP-reinforced concrete flat slabs. They found that the model gives excellent correlation with test results of slabs reinforced with FRP reinforcing bars.

REFERENCES

30. Theodorakopoulos, D. D., and Swamy, R. N., "Ultimate Punching Strength Analysis of Slab-Column Connections," *Cement and Concrete Composites*, V. 24, No. 6, 2002, pp. 509-521.

31. Theodorakopoulos, D. D., and Swamy, R. N., "Analytical Model to Predict Punching Shear Strength of FRP-Reinforced Concrete Flat Slabs," *ACI Structural Journal*, V. 104, No. 3, May-June 2007, pp. 257-266.

AUTHOR'S CLOSURE

The author would like to thank the discussers for their interest in the paper and for their encouraging words about the ideas of the critical shear crack theory.

Closure to discussion by Windisch

The sketch of Fig. 2 is a physical explanation of how the development of the critical shear crack influences the behavior of the slab, allowing to understand, for instance, the decompression of the soffit of a slab measured during testing. As the discusser may note, no quantitative, only phenomenological, explanations are obtained from this figure.

The same happens with respect to Fig. 3. It explains the influence of tangential cracking and of its location on punching shear strength. The model itself, however, deals with ordinary (orthogonal) reinforcement layout for which the failure criterion of Fig. 5 is proposed.

Closure to discussion by Subramanian

The value of mR_d (design moment capacity per unit width) can, for instance, be calculated according to ACI 318-08, Sections 10.2 and 10.3. The assumptions on the shape discussed in Section 10.2.6 have limited influence on the value of the design moment capacity for typical reinforcement ratios.

Disc. 105-S43/From the July-August 2008 *ACI Structural Journal*, p. 451

Design and Analysis of Heavily Loaded Reinforced Concrete Link Beams for Burj Dubai. Paper by Ho Jung Lee, Daniel A. Kuchma, William Baker, and Lawrence C. Novak

Discussion by Andor Windisch

ACI Member, PhD, Karlsfeld, Germany

STRUT-AND-TIE MODEL USED IN LINK BEAM

The authors are to be complimented for their interesting paper. What is the "speciality" of the strut-and-tie model shown in Fig. 5, where the reader might perceive that this is a D-region? According to MacGregor[16] "In D-regions...a major portion of the load is transferred directly to the supports by in-plane compressive forces in the concrete and tensile forces in reinforcement and a different design approach is needed." How was the horizontal position of the C-C-C nodes found that resulted in the θ = 39.1-degree strut inclination? Nor is it not clear when a bottle-shaped or a narrow bottle-shaped strut or a uniform field of diagonal compression throughout a deep beam shall be assumed. A "direct" design looks different.

NONLINEAR FINITE ELEMENT ANALYSIS

The load and boundary conditions shown in Fig. 8 do not properly model the real conditions: along the (horizontal) boundary cross sections of the walls, significant bending moments (besides normal and shear forces) act that can considerably influence the load-bearing capacity of the link beam. Reference should be given to the predicted crack patterns shown in Fig. 10—under the opening moments affecting the wall sections, much more pronounced cracked regions would have been found.

For the validation of the concrete material models of the three programs, a test[14] under monotonic loading was used. Following are some questions and comments:

- The link beams in the tower are subjected to wind loads from different directions. This alternating load results in pronounced cracking in the relevant tension region that becomes the compression zone in the next loading phase. Did the concrete material model consider this effect? That is a further reason why more realistic boundary conditions should have been chosen.
- The situation under seismic loads is much more dramatic. Did the authors consider this issue in the design?
- The three predicted load-deformation responses (Fig. 7) are close to each other; nevertheless, they overestimate the failure load quite substantially. (As the load-deformation response of the test specimen is not shown, it is not clear whether the predicted response was close enough to the measured one.) Did the nonlinear finite element models at least predict the type of failure properly? For a designer, the most important aspect is the load-bearing capacity. What criterion can be formulated for the finite element analysis to indicate failure?

DISCUSSION OF PREDICTED LINK BEAM BEHAVIOR

The predicted crack patterns displayed in Fig. 10 show a pronounced opening corner effect with inclined cracks around the corners. This opening-corner effect should have been considered in the strut-and-tie model. (Until now, after more than 30 years of development, no valid strut-and-tie model has been developed for opening corners at all. Even MacGregor[16] does not give any assistance.)

The predicted cracking shown in Fig. 18 reveals that horizontal web reinforcement would be as efficient as the vertical stirrups, especially in the neighborhood of the pier walls. The strut-and-tie model focuses only on vertical ties as shear reinforcement, whereas horizontal web reinforcement is never referred to.

CONCLUSIONS

1. The reported effect of the pier walls could be less advantageous if the real loading effects would have been considered in the model. The reversed loading could have even more detrimental influences;

2. A more detailed analysis (if the model is correct) deserves a more economical solution compared to a much quicker (and cheaper) calculation model, that is, the model in ACI 318-99;

3. Brown and Bayrak[17] emphasized that "the use of the current provisions for STM in both ACI 318-05 and AASHTO LRFD does not produce adequate levels of safety." Who is right?

4. The authors are right. It is well known (nevertheless, systematically neglected by the users of strut-and-tie modeling) that in D-regions, more longitudinal flexural reinforcement is needed as advised by strut-and-tie modeling where the internal lever arm is regularly taken as 0.9d, even if the region is prestressed, which increases the depth of the compression zone; and

5. The discusser strongly doubts whether the code provisions cited would be valid for link beams under alternating loading such as in the Burj Dubai.

REFERENCES

16. MacGregor, J. G., "Derivation of Strut-and-Tie Models for the 2002 ACI Code," *Examples for the Design of Structural Concrete with Strut-and-Tie Models*, SP-208, K. Reineck, ed., American Concrete Institute, Farmington Hills, MI, 2002, pp. 7-40.

17. Brown, M. D., and Bayrak, O., "Design of Deep Beams Using Strut-and-Tie Models—Part II: Design Recommendations," *ACI Structural Journal*, V. 105, No. 4. July-Aug. 2008, pp. 405-413.

Disc. 105-S43/From the July-August 2008 *ACI Structural Journal*, p. 451

Design and Analysis of Heavily Loaded Reinforced Concrete Link Beams for Burj Dubai. Paper by Ho Jung Lee, Daniel A. Kuchma, William Baker, and Lawrence C. Novak

Discussion by Kent A. Harries

FACI, William Kepler Whiteford Faculty Fellow and Assistant Professor, Department of Civil and Environmental Engineering, University of Pittsburgh, Pittsburgh, PA

The discussed paper presents varied analyses of very large link or coupling beams coupling the walls of the Burj Dubai tower. The link beams are clearly shear critical, having their design moment capacity determined as $M = VL/2$, where V is the design shear and L is the span of beam. Based on the nature of coupled wall structures, the large shear forces induced in the beams result from lateral loads applied to the structure. The beams permit the individual wall piers to act as a unit; thus, lateral forces are resisted by a combination of cantilever wall pier action and an axial couple generated between walls resulting from the frame action imparted by the beams.

The analyses and discussion presented by the authors appear to suggest the use of the strut-and-tie method to overcome what is suggested to be the restrictive shear stress limits on these members imposed by ACI 318. The reviewer is concerned that this conclusion, while correctly deduced from the authors' work, is nonetheless erroneous and potentially dangerous with respect to the behavior of coupled high-rise structures. The primary reason for these misleading conclusions is that the authors have considered only the case of a monotonically loaded beam. The following brief discussion refutes the findings of the discussed paper as they relate to high-rise coupled wall structures.

Conventionally reinforced concrete coupling beams are recognized to be susceptible to sliding shear failure at the beam-wall interface.[18,19] Sliding shear is described as follows.[20]

"Under reversing loads, intersecting cracks propagate across the entire depth of the beams at their ends. As subsequent inelastic load reversals are applied, concrete at the ends [is] destroyed by cracking, abrasion and spalling. With the concrete destroyed, shear transfer by 'truss action' is not possible and the transverse hoops become ineffective. Interface shear transfer is lost. Eventually, dowel action of longitudinal reinforcement [provides] the primary shear resistance… Deterioration of the concrete at the ends of the beams [is] intensified by elongation of the beams, caused by residual tensile strains in the longitudinal reinforcement. These strains developed with successive load reversals into the inelastic range."

Sliding shear at the face of the wall begins to affect the response of conventional beams having shear stresses in the range of $4\sqrt{f_c'}$ to $6\sqrt{f_c'}$ psi ($0.3\sqrt{f_c'}$ to $0.5\sqrt{f_c'}$ MPa). The failure of the Mount McKinley Building during the 1964 Anchorage Earthquake[21] is an often-cited example illustrating the shortcomings of conventionally reinforced coupling beams.

By providing intermediate midheight longitudinal bars, the hysteretic response is improved (through additional dowel action) and strength deterioration due to shear is delayed, although not mitigated.[22-24] Beams with intermediate bars do not perform well when the shear stress is greater than $6\sqrt{f_c'}$ psi ($0.5\sqrt{f_c'}$ MPa). Providing cranked diagonal reinforcement near the beam ends has been shown to improve the hysteretic behavior by preventing sliding shear and by spreading the hinging regions away from the wall face.[25,26] This detail, however, poses construction difficulties and results in extra cost. Additionally, designers may avoid this detail because it is not explicitly covered in ACI 318. Similarly, the use of high-strength concrete[27,28] or fiber-reinforced concrete[29] has shown some improvement in delaying the occurrence of sliding shear.

Diagonally reinforced coupling beams exhibit better performance[19,30] and theoretically overcome limits imposed by concrete shear capacity. As demonstrated by Harries et al.,[31] however, the design of diagonally reinforced beams becomes largely impractical for all but the shortest beams at gross section shear stresses exceeding approximately $6\sqrt{f_c'}$ psi ($0.5\sqrt{f_c'}$ MPa).

There are three methods by which sliding shear may be avoided:

1. Reduce the shear stress in the beam. This may result in impractically large coupling beam cross sections[31];

2. Provide diagonal reinforcement. Diagonal reinforcement is perhaps the only successful solution for reducing the potential for sliding shear and enhancing the hysteretic characteristics of coupling beams having span-depth ratios as large as 3.33.[32] Steel placement in diagonally reinforced beams having span-depth ratios greater than 1.5, however, is generally impractical[31]; and

3. Provide a steel or hybrid coupling beam[33,34] as reportedly was done for the more heavily loaded Beams LB3 and LB4 in the Burj Dubai.

Conventionally reinforced concrete coupling beams having relatively high magnitudes of shear stress should be expected in practice. A review of the experimentally observed behavior of such beams reveals that strains in the longitudinal reinforcement barely achieve yield prior to the onset of sliding shear.[18,20,24,35] In cases where conventional reinforcement was used in beams having span-depth ratios less than 1.5, the beams were unable to achieve the loads for which they were designed prior to the onset of sliding shear.[18,24]

While the strut-and-tie approach would appear to permit greater capacities to be achieved, the behavior of the structural system must be accounted for and results from previous work, particularly experimental results, cannot be overlooked. In this case, the discusser maintains that the conclusions of the discussed paper are incorrect in context. Furthermore, the discusser has some concern for the LB2 beams that have been reportedly used in the Burj Dubai. Finally, there is a minor typographical error in Table 1: the design moment for LB2 = 1964 kN.

REFERENCES

18. Paulay, T., "Coupling Beams of Reinforced Concrete Shear Walls," *Journal of the Structural Division*, ASCE, V. 97, No. ST3, 1971, pp. 843-862.

19. Paulay, T., and Binney, J. R., "Diagonally Reinforced Concrete Beams for Shear Walls," *Shear in Reinforced Concrete*, SP-42, American Concrete Institute, Farmington Hills, MI, 1974, pp. 579-598.

20. Barney, G. B., et al., "Earthquake Resistant Structural Walls Test of Coupling Beams," *Report* to NSF, submitted by Portland Cement Association, Research and Development, Skokie, IL, 1978.

21. Berg, V. B., and Stratta, J. L., "Anchorage and the Alaska Earthquake of March 27, 1964," AISC, New York, 1964, 63 pp.

22. Aktan, A. E., and Bertero, V. V., "Seismic Response of R/C Frame-wall Structures," *Journal of the Structural Division*, ASCE, V. 110, No. ST8, 1984, pp. 1803-1821.

23. Scriber, C. F., and Wight, J. K., "Delaying Shear Strength Decay in Reinforced Concrete Flexural Members under Large Load Reversals," *Report* UMEE 78 R2, Department of Civil Engineering, University of Michigan, Ann Arbor, MI, 1978.

24. Tassios, T. P.; Moretti, M.; and Bezas, A., "On the Coupling Behavior and Ductility of Reinforced Concrete Coupling Beams of Shear Walls," *ACI Structural Journal*, V. 93, No. 6, Nov.-Dec. 1996, pp. 711-720.

25. Paparoni, M., "Model Studies of Coupling Beams," *Proceedings of the International Conference on Tall Concrete and Masonry Buildings*, V. 3, 1972, pp. 671-681.

26. Aristizabal-Ochoa, J. D., "Seismic Behavior of Slender Coupled Wall Systems," *Journal of the Structural Division*, ASCE, V. 113, No. ST10, 1987, pp. 2221-2234.

27. Bristowe, S., "Seismic Response of Normal and High-Strength Concrete Members," PhD dissertation, McGill University, Montreal, QC, Canada, 2000, 244 pp.

28. Xiao, Y.; Esmaeily-Ghasemabadi, A.; and Wu, H., "High-Strength Concrete Short Beams Subjected to Cyclic Shear," *ACI Structural Journal*, V. 96, No. 3, May-June 1999, pp. 392-399.

29. Canbolat, B. A.; Parra-Montesinos, G. J.; and Wight, J. K., "Experimental Study on Seismic Behavior of High-Performance Fiber-Reinforced Cement Composite Coupling Beams," *ACI Structural Journal*, V. 102, No. 1, Jan.-Feb. 2005, pp. 159-166.

30. Shiu, N. K.; Barney, G. B.; Fiorato, A. E.; and Corley, W. G., "Earthquake Resistant Walls—Coupled Wall Test," *Report* to NSF, Portland Cement Association, Research and Development, Skokie, IL, 1981.

31. Harries, K. A.; Fortney, P.; Shahrooz, B. M.; and Brienen, P., "Design of Practical Diagonally Reinforced Concrete Coupling Beams—A Critical Review of ACI 318 Requirements," *ACI Structural Journal*, V. 102, No. 6, Nov.-Dec. 2005, pp. 876-882.

32. Aktan, A. E., and Bertero, V. V., "The Seismic Resistant Design of R/C Coupled Structural Walls," *Report* No. UCB/EERC81/07, Earthquake Engineering Research Center, University of California-Berkeley, Berkeley, CA, 1981.

33. Harries, K. A.; Gong, B.; and Shahrooz, B., "Behavior and Design of Reinforced Concrete, Steel and Steel-Concrete Coupling Beams," *Earthquake Spectra*, V. 16, No. 4, Nov. 2000, pp. 775-800.

34. Harries, K. A., and Shahrooz, B., "Hybrid Coupled Wall Systems," *Concrete International*, V. 27, No. 5, May 2005, pp. 45-51.

35. Galano, L., and Vignoli, A., "Seismic Behavior of Short Coupling Beams with Different Reinforcement Layouts," *ACI Structural Journal*, V. 97, No. 6, Nov.-Dec. 2000, pp. 876-885.

AUTHORS' CLOSURE

The authors appreciate the discussions provided by Windisch and Harries. The authors will first address the concern raised by Harries, and shared by Windisch, that the design approach used in the Burj Dubai and the analytical validation was not suitable for beams subjected to significant load reversals. The authors will then address the additional comments of Windisch.

In the paper, the authors stated that "Due to the tapering of the tower, the primary demand on the link beams is from gravity load redistribution, flow from the taller core to the perimeter of the structure." The largest shear demands are in the beams at the location of these setbacks where there is not the concern for the type of load reversal or opposite direction shear cracking raised in the discussions. Harries' comments are premised by his assumption that "Based on the nature of coupled wall structures, the large shear forces induced in the beams result from lateral loads applied to the structure." Thus, the concerns raised by Harries are not applicable to the link beams that were the subject of this paper. The authors agree with the technical arguments presented and summarized by Harries that would apply to link beams whose demands are governed by lateral loadings. One of the authors is presently engaged in testing a large multi-story reinforced concrete coupled wall structure that was designed to resist cyclic lateral loading from seismic actions. In this test structure, diagonal reinforcement has been used for the reasons given in Harries' discussion.

This response is also considered to address the concerns of Windisch regarding the influence of significant reverse loading on the design and performance of link beams. Because two ACI members both raised this concern, the authors should have better anticipated that many readers would naturally assume that the dominant shear demands were from lateral loads. Thus, the authors should have been more emphatic about the source of the demands for the link beams in Burj Dubai.

The other comments of Windisch were on the following topics: the shape of the strut-and-tie model, the appropriateness of the selected finite element model, comparisons with test data, the criteria used to assess the predicted capacity, cracking patterns, and the role of horizontal reinforcement.

As presented in Fig. 5, the shape of the strut-and-tie model was selected so that the full shear force would need to be lifted up over the length of the link beam, as opposed to having a portion of the shear flow along a diagonal strut that runs from one wall pier to the other pier. The strut-and-tie design philosophy permits the designer to use any admissible shape for the truss model; the designer selected what was considered to be a conservative design that also provided substantial vertical reinforcement to resist bursting forces in the middle region of the link beam. In response to the specific question of the horizontal position of the CCC node, it was selected to provide sufficient width to support the vertical force V_u given in Fig. 5.

In the nonlinear finite element model presented in Fig. 8, only a segment of the surrounding pier walls was modeled. In the Burj Dubai, the wall piers were sufficiently large so that the bending of these walls was insignificant and thereby not a factor that was considered to affect the behavior of the link beams. The test result presented in Fig. 7 was from a beam subjected to cyclic loading and not the type of monotonic situation in the Burj Dubai. Thus, the use of this test data to validate the computational model was a conservative approach.

The matter of what criteria to use for determining the capacity predicted by a nonlinear finite element analysis is a critically important issue for the use of computational tools for design validation. Unfortunately, there is not a clear set of criteria that can be applied to these analytical predictions for assessing capacity due to the dependency of these predictions on differences in the capabilities and limitations of existing material and behavioral models, and how they have been employed in computational tools and in the development of finite element models in any specific investigation. Consequently, assessing a reliable capacity from a computational tool requires the conduct of sensitivity analyses to investigate the influence of modeling decisions on the predicted capacity and behavior so that conservative yet realistic assumptions can be employed in the final, selected model to be used in the study. It also involves using failure criteria that are specific to the models being used. For example, in the predictions by VecTor2 that account for the influence of compression softening, for each element the ratio of principal compressive stress to a compressive strength (dependent on the principal transverse tensile straining) was examined so that the determined reliable capacity was well below the point in which crushing would be expected.

As pointed out by Windisch, the extensiveness of corner cracking is a significant factor to consider in the selection of the shape of the strut-and-tie model to use in design. The model presented in this paper was chosen to take this pattern of cracking into consideration. It is certainly possible to imagine a different model in which the designer relied on the transfer of shear over the full depth of the interface between the link beam and wall pier. Given the range of application of the strut-and-tie design methodology, designers should be encouraged to consider the location and extent of cracking as is being suggested by Windisch. Nonlinear finite element analysis tools can be effective means of predicting this cracking.

Windisch also comments on the role of horizontal reinforcement. The authors agree that the effect of this horizontal reinforcement is not captured by the selected strut-and-tie model, but its role is illustrated in the predictions of nonlinear finite element tools. The role of horizontal reinforcement has been captured in studies and strut-and-tie models for the flow of forces in deep beams.

The authors have not commented on the work by Brown and Bayrak as providing a public critique of their work in response to this discussion; it was considered outside the limits of this response. It is useful to note that while the general applicability of the strut-and-tie method is a great strength, any assessment of the conservatism of this approach greatly depends on the specific geometry and loading of the structure and the selected shape of the strut-and-tie model.